

# Area Law Violations in Entanglement Measures for Spatially Inhomogeneous Quantum Spin Chains

AC38091

September 2022

## Abstract

In this report, we investigate the scaling of measures of entanglement in one dimensional, inhomogeneous quantum spin chains. In particular, we reproduce key findings on entanglement entropy and logarithmic negativity in spatially inhomogeneous system, and extend the analytical results to systems with slowly decaying couplings. We verify these results with the exact solution (in the case of quadratic models) and the Strong Disorder Renormalisation Group (SDRG) method in the case of interacting models for which an exact solution is not possible. We show that with slowly decaying couplings, the area law violation is maintained but the system approaches a simple disordered system in the large subsystem limit.

## Contents

<b>1</b>	<b>Introduction</b>	<b>3</b>
<b>2</b>	<b>Literature Review</b>	<b>5</b>
2.1	Area Law Violations in Quantum Systems . . . . .	5
2.2	Measures of Entanglement . . . . .	5
2.3	SDRG Procedure . . . . .	6
<b>3</b>	<b>Measures of Entanglement</b>	<b>8</b>
3.1	Entanglement as a Information Phenomenon . . . . .	8
3.2	Entanglement Entropy and Negativity . . . . .	8
<b>4</b>	<b>The Random Inhomogeneous Chain and the SDRG method</b>	<b>10</b>
4.1	Random Inhomogeneous 1D Chain . . . . .	10
4.2	SDRG Procedure . . . . .	10
4.3	SDRG Flow . . . . .	10
<b>5</b>	<b>Algorithmic Implementation and Complexity</b>	<b>12</b>
<b>6</b>	<b>Existing Results and Verification</b>	<b>14</b>
6.1	Entanglement Entropy . . . . .	14
6.2	Logarithmic Negativity . . . . .	14
6.3	Randbow Chain . . . . .	16
6.4	Randbow Subregion Analysis . . . . .	18
6.5	Randbow Chain Exact Solution . . . . .	19
<b>7</b>	<b>Entanglement negativity for the randbow chain</b>	<b>22</b>
7.1	Analytical expectation . . . . .	22
7.2	SDRG results . . . . .	22

<b>8</b>	<b>Power law systems</b>	<b>26</b>
8.1	Power law systems: analytical expectations . . . . .	26
8.2	Entanglement Entropy: SDRG and exact results . . . . .	26
8.3	Logarithmic negativity scaling . . . . .	27
<b>9</b>	<b>Conclusion</b>	<b>32</b>
9.1	Logarithmic negativity for the Randbow system . . . . .	32
9.2	Entanglement scaling for the power-law system . . . . .	32
9.3	Limitations and Future Work . . . . .	32
<b>A</b>	<b>Quantum Mechanics: A Brief Summary</b>	<b>33</b>
A.1	States and Amplitudes . . . . .	33
A.2	Normalisation and Unitary Operators . . . . .	33
A.3	Time Evolution . . . . .	34
A.4	Observables . . . . .	34
A.5	Hamiltonians and Groundstates . . . . .	34
A.6	Commutators . . . . .	35
A.7	Spin . . . . .	35
<b>B</b>	<b>Exact Solution to Non-Interacting Case</b>	<b>36</b>
B.1	The Jordan-Wigner Transformation . . . . .	36
B.2	Using the JW transformation in the exact solution . . . . .	36

# 1 Introduction

Entanglement is often regarded as ‘the’ stylistic feature of quantum systems [1]. In recent years a significant amount of work has gone into quantifying the *scaling* of the entanglement entropy:

$$S(\rho) = -\text{Tr}(\rho \log \rho) \quad (1.1)$$

and of the logarithmic negativity:

$$\varepsilon(\rho_A) = \ln \|\rho_A^{T_2}\| \quad (1.2)$$

of a subsystem defined by a partial density matrix  $\rho_A$ <sup>1</sup>. In particular, this report will extend the work of two papers ([1] and [2]) which quantified the scaling of both of these entanglement measures in a variety of settings. In particular, they studied the entanglement scaling of one dimensional quantum spins chains with varying degrees of heterogeneity, starting from the centre of the spin chain.

Quantum spin chains are (in)finitely long collections of quantum spins in one dimension. Whilst a one dimensional system may seem like a trivial object of study, one dimensional chains provide a first step towards more detailed models of higher dimensional systems (see for example [3]), and particular one dimensional quantum systems have been used to study 1+1 dimensional classical systems [4]. There are of course genuinely one dimensional systems of interest [5], and simple, one dimensional classical spin chains are solvable via transfer matrices [6].

However, apparent inconsistencies have arisen in the predicted scaling of entanglement observables and their numerically observed outcomes [7]. In particular, it is known that for gapped, spatially invariant systems, entanglement entropy must scale with an area law [8]. An interesting research programme began in 2004 [7] to study what changes to the system Hamiltonian would result in area law violations, to exact volume scaling or logarithmic scaling. Subsequent research ([9], [1], [2]) has developed a significant pool of results including by enforcing a degree of spatial inhomogeneity through couplings that decay from the centre.

To motivate this research programme in area law violations, Eisert et al. [10] list four important motivations for studying measures of entanglement:

1. Black hole physics: Beckstein-Hawking radiation is proportional to the boundary of the black hole [11].
2. The theory of long range quantum correlations - is it possible to have arbitrarily long range quantum correlations away from criticality?
3. Complexity of numerical simulation: great success has been made in classical physical through mean field theory to more efficiently simulation and solve complex systems ([12]). If we understand how and when mean field theories work for quantum systems, this will help us to effectively model and solve complex quantum systems.
4. Topological entanglement entropy, a novel order parameter, cannot be described by local conditions.

In this report, we will investigate the scaling of two measures of entanglement, entanglement entropy and entanglement negativity, with varying degrees of spatial inhomogeneity. We will verify prior results for spatially inhomogeneous systems and systems whose couplings decay exponentially, before extending some results for exponential systems to negativity and investigating a new type of inhomogeneity that decays more slowly than in exponential systems. This will be a direct extension to the work reported in [1] and [2].

The presence of disorder introduces a new richness of modelling possibilities but also creates serious technical problems. In particular, local spatial homogeneity is violated and this loss of symmetry makes solving the models more difficult. This has prompted a wave a numerical techniques based on

---

<sup>1</sup>For definitions and details, see section 3.2

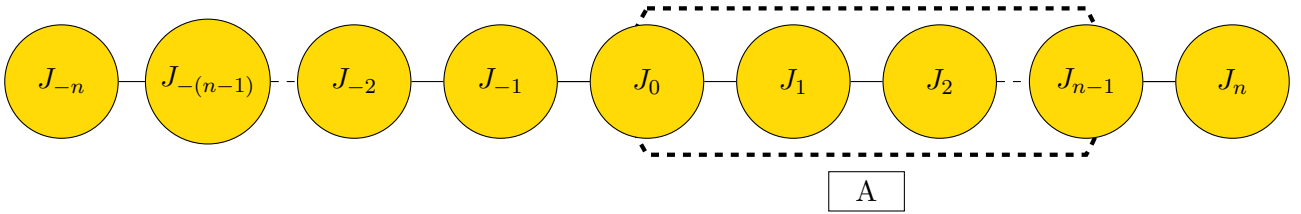


Figure 1.1: A chain of spins with the central spin labelled  $J_0$ . The subsystem  $A$  is highlighted with the dashed line. Unless otherwise stated, subsystems will always start from the centre of the chain.

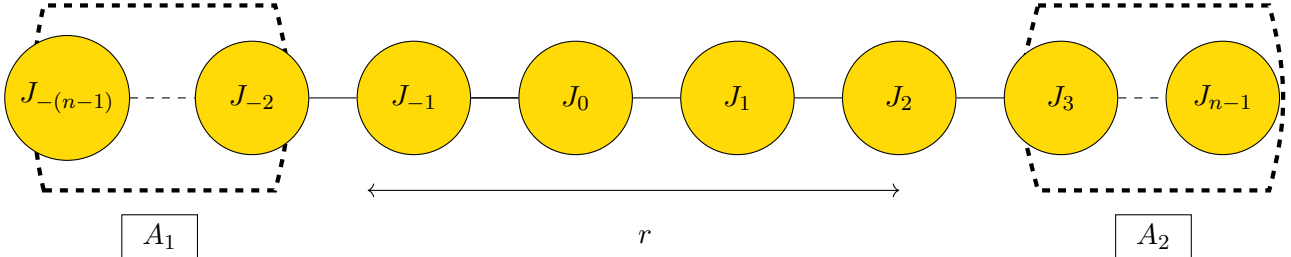


Figure 1.2: A chain of spins with a pair of disjoint subsystems, separated by a distance  $r$ . The subsystems  $A_1$  and  $A_2$  are highlighted with the dashed line. Unless otherwise stated, subsystems will always start from the centre of the chain.

renormalisation group theory ([13], [7]). Further complicating the picture is the presence of interactions. The combination of disorder and interactions makes disordered quantum chains truly complex system: there are no known analytical solutions to the interacting disordered spin chain [1]. We will implement some analytical results, but to facilitate analysis we use the Strong Disorder Renormalisation Group (SDRG) technique for the majority of our calculations. The SDRG technique in particular is useful for understanding the groundstate of disordered systems and is known to be asymptotically exact [7]. We implement algorithms for the SDRG procedure and associated analyses, as well as for the exact solutions where possible, at arbitrary precision.

In this report, we will frequently refer to a ‘subsystem’ centred in a one dimensional chain. For consistency, we present in figures 1.1 and 1.2, the two key subsystem scenarios. In figure 1.1, we show a single subsystem  $A$  in the centre of the chain. The details of the setup will depend on the boundary conditions and the parity of the system length  $L$  - in particular, whether  $J_0$  is in the centre of the chain or to the right hand side of the central coupling. In figure 1.2, we show two disjoint subsystems separated by a region  $r$ , which will normally be restricted to even length. Again, the exact implementation will depend on the boundary conditions and the parity of the system’s length.

Throughout, we will use  $J_i$  to refer to the  $i^{\text{th}}$  site as well as the bond immediately to the right of said bond. In ambiguous cases we will clarify things accordingly. In the case of periodic boundary conditions, the bond extending from site  $L$  will connect around into site 1. In open boundary conditions, site  $L$  will have a bond  $J_L = 0$  which effectively eliminates that interaction from the system.

The layout of the rest of this report is as follows: In section 2, we review current literature around area law violations in quantum systems and the SDRG procedure. In section 3, we cover different measures of quantum entanglement and the difference between entanglement entropy and negativity. In section 4, we will lay out the spin chain models to be investigated and the SDRG procedure. In section 5, we will briefly review the implementation of the SDRG procedure and demonstrate some initial verifications. In section 6 we will verify some existing results for area law violations, and in sections 7 through 8, we will demonstrate the new results on entanglement negativity for old systems and for the new slowly decaying systems. Lastly, in section 9 we will evaluate the new results and discuss areas for further research. In the appendices, we review basic quantum physics and mathematics in A and the Jordan-Wigner transformation in B.

## 2 Literature Review

### 2.1 Area Law Violations in Quantum Systems

We will briefly survey the wide literature of area law violations in quantum systems. For a thorough review, we recommend [10]. Early work on the scaling of entropy in quantum systems focused on the study of black holes: in particular, Bombelli et al. [14] and Srednicki [15]. As discussed in section 1, the horizon of a black hole and the theory of Hawking radiation are of great general interest. Srednicki argued that for a field of quantum harmonic oscillators divided into a spherical ‘in’ region and exterior, the entropy of the ‘in’ region must scale with the area as opposed to the volume, as the surface area is the only region common to both subregions. In 2004 Hastings published a proof of the area law for strictly local systems [8], e.g. Hamiltonians of the form:

$$H = \sum_{i=1}^N H_{i,i+1} \quad (2.1)$$

where  $H_{i,i+1}$  is a function only of the sites  $i$  and  $i+1$ , and this was followed by a more general proof in 2005 by Eisert et al. [16]. By [17] it was well established that for local, gapless hamiltonians, the ground state had an entropy that scaled with the area rather than the volume.

This ‘area law’ sets the baseline for the physics of such systems: any evidence of violations to this area law must also explain how to account for this violation. Many theoretical systems do in fact display area law violations of their quantum entropy [18], and thus a literature has sprung up to identify and explain these phenomena with a variety of tools. For example, in a very detailed survey Calabrese and Cardy [19] give a thorough treatment through  $(1+1)d$  conformal field theory (CFT) of the entanglement entropy, and show that the entropy  $S_A$  of a subsystem  $A$  of length  $l$  at zero temperature in an infinitely long, 1D system without boundaries is:

$$S_A \sim (c/3) \log(l/a) \quad (2.2)$$

where  $c$  is the central charge and  $a$  is the lattice spacing. This is known as a *logarithmic correction* to the area law.

Page [20] shows with an information theoretic argument that does not use the harmonic oscillator framework that progressively smaller subsystems contain virtually no information on the total system, which may explain the logarithmic scaling: as the subsystem size decreases (and as the number of subsystems increases), the entropy decreases more and more quickly, giving rise to the logarithmic scaling in  $l$ . Furthermore, area law violations do not just come in via the subsystem length. With a combination of analytical and approximate results (more on SDRG below in 2.3) Giampaola et al. show that the system size  $N$  also affects the entanglement scaling, especially under certain open conditions [21].

Most of the references above report on the entanglement entropy (see 3.2 for a definition), but results are not limited to this. For example, Calabrese et al. compute the scaling of the logarithmic negativity in the CFT framework [22].

Given that the locality of the Hamiltonian and the boundary conditions affect the scaling, the working hypothesis is that the violations come from a degree of spatial inhomogeneity in certain systems. For example, in a random coupling spin chain, there will be small areas that are deeply inhomogeneous, and these contribute positively to the entropy in a way that a homogeneous model would not. This leads directly to the experiments discussed in [1].

### 2.2 Measures of Entanglement

A proper physical and mathematical treatment of measures of entanglement will be given in section 3. Here we will review the recent literature on measures of entanglement in quantum mechanics. An excellent review is [23], section two. As a starting point, Bell [24] presents his ‘game’ in which Alice and Bob attempt to coordinate their observations of a potentially entangled pair of particles. A full illustration is beyond the scope of this paper, but it can be shown (ibid) that under certain conditions

(see below on the CHSH inequality) this game is properly ‘entangled’, in that the (classical) states of both particles are not known until either one is measured.

This was developed into the CHSH inequality [25], which is now a benchmark test for entangled states. In Vedral et al. 1997, a set of axioms for entanglement to satisfy is presented [26] to provide a rigorous grounding for entanglement. This is in response to the fact that states had been found that did not violate the CHSH inequality (i.e. they did not appear to be entangled) but that were effectively entangled under local operations and classical communication (LOCC, again see section 3.1) [27]. However, there is a tradeoff between what is often called the ‘operational’ view of entanglement, which measures entanglement in a way that is physically intuitive, and the mathematical approach that seeks rigorous and numerically stable measures ([4], [28]). For example, the entanglement of distillation gives the number of maximally entangled pairs that can be purified from a given quantum state [29]. Yet purification processes are varied and there is not yet a way of calculating this quickly. On the other hand, negativity (see section 3.2 for a definition) is well defined but does not have any obvious physical interpretation. Mathematically, perhaps the most important criteria for any measure of entanglement is that it is *monotone* [28], i.e. that for any measure  $E$  on a density matrix  $\rho$  we have:

$$E(\rho) \geq \sum_i p_i E(p_i) \quad (2.3)$$

Which implies that any classical interference with the state (represented by the classical probability weightings  $p_i$ ) can only lower its entropy. This is one requirement for keeping measures of entropy focused strictly on the quantum correlations.

Single measures of entanglement have also been extended to a complete *entanglement spectrum* [30], which is in turn related to moments of the reduced density matrix (ibid, [1]). The moments of the reduced density matrix are given by its eigenvalues  $\lambda_i$  as follows:

$$R_\alpha = \sum_i \lambda_i^\alpha \quad (2.4)$$

Which are in turn the object of all numerical approaches that depend on matrix product states (see section 2.3 below for more information).

## 2.3 SDRG Procedure

Whilst in non-interacting cases, one dimensional spin chain models are often analytically solvable, this is not the case in general. This observation of course holds for more such quantum systems, and the renormalisation group (RG) approach to approximating complex systems (quantum and classical) came out of work with (Michael) Fisher and Wilson in the 1960s [31]. The renormalisation group approach involves successively integrating out the strongest factors in a model to approach a state that is accurate *even at a critical point*. Typically, order parameters will diverge in a scale free manner, i.e. according to a power law, which gives rise to fluctuations with no specific scale. This scale invariance is difficult to capture with traditional mathematical methods, and hence the RG method has proven so useful.

In this paper we will focus exclusively on *disordered* models, which puts us in the domain of the *strong disorder renormalisation group* (SDRG). For a very thorough review, see [32] and [33]. Studies of disordered systems start as early as [34], who showed that the experimental magnetisation of certain materials could be smooth even around the critical point, and that this was explainable by a degree of disorder. The key contribution was from Dasgupta, Ma, and Hu ([35], [36]) who defined a rule for the elimination of bonds that was generalised by (Daniel) Fisher [13]. Since then the SDRG procedure has been used to investigate a great variety of challenging disordered problems ([37], [38], [39], [7], [9], [1], [2]).

The SDRG procedure is often used in complement (or contrast) to matrix product states, and in particular to the density matrix renormalisation group (DMRG)[40]. For a thorough review, see [41] and [42]. A detailed discussion of the literature on DMRG is beyond the scope of this report, but it is crucial out that in [1], the DMRG technique struggled to converge for large system size  $L$ , with

significant errors relative to the exact solution (where exact solutions were not available). For this reason we have not used the DMRG method in this report.

### 3 Measures of Entanglement

#### 3.1 Entanglement as a Information Phenomenon

Entanglement is a type of correlation unique to quantum mechanics, but defining the style of correlation is difficult. One approach is the ‘operational approach’ [4], which says that states are entangled if and only iff (iff) they are *seperable*. Seperability implies that, given a set of classical probabilities  $\{p_i\}$ , and a similar set of density matrices for two subsystems  $A$  and  $B$ , the final density matrix  $\rho$  can be written as:

$$\rho = \sum_i p_i \rho_A^i \otimes \rho_B^i \quad (3.1)$$

Thus a first (and incorrect) attempt would be to define entanglement as ‘the property of any statement that cannot be reached by local operations and classical communication’ (LOCC). LOCC includes, for example, experiments on quantum systems to take observations (see A.1), and traditional methods of communication (Alice: ‘Bob, my spin is in state  $|\psi\rangle$ , how about you?’). However, as Peres shows [43], LOCC is only a subset of operations that lead to separable states. Rather, density matrices must be at least *positive partial transpose preserving*: this is known as the Peres criterion. The partial transpose is defined as follows - given a density matrix  $\rho$  defined as:

$$\rho = \sum_{ijkl} p_{kl}^{ij} |i\rangle \langle j| \otimes |k\rangle \langle l| \quad (3.2)$$

Then the partial transpose with respect to B is:

$$\rho = \sum_{ijkl} p_{kl}^{ij} |i\rangle \langle j| \otimes (|k\rangle \langle l|)^T \quad (3.3)$$

The preceeding matrix is positive iff it does not have any negative eigenvalues.

Whilst the Peres criterion is strictly correct, LOCC presents a useful heuristic for defining a set of axioms that any measure of entanglement must satisfy [26]. There is significant debate over what a minimal set of such axioms should be. Following [4], we use the following three necessary conditions for a good measure of entanglemnt  $E$ :

1. *Monotonicity*:  $E(\rho) \geq \sum_i p_i E(p_i)$  (see section 2.2)
2. *Convexity*:  $\sum_i p_i E(\rho_i) \geq E(\sum_i p_i \rho_i)$
3. *Additivity under the tensor product*:  $E(\otimes_i \rho_i) = \sum_i E(\rho_i)$

The additivity requirement is exceptionally useful as it allows the calculation of product states, including the random singlet phase that will be discussed in 4.2. The convexity requirement is perhaps the only one that can be considered contentious. The right hand side of the convexity condition describes a *mixed state*, i.e. a classical combination of quantum states. The way that measures of entanglement deal with mixed states is crucial [4]. Convexity implies that a classical mixing of states cannot produce entanglement, which is *prima facie* a desirable property of an entanglement measure. However, Plenio shows that for entanglement negativity (see below, section 3.2) the monotonicity requirement is sufficient to guarantee its suitability as a measure of entanglement because ‘convexity is merely a mathematical requirement for entanglement monotones and generally does not correspond to a physical process describing the loss of information’ [28]. For general measures of entanglement, however, it would be important to revisit the convexity requirement.

#### 3.2 Entanglement Entropy and Negativity

We will now define the key measures of entanglement used in this report. Firstly, we define the general Rényi entropies:



$$S_n(\rho_A) = \frac{1}{1-n} \log \text{Tr} \rho_A^n \quad (3.4)$$

where  $\rho_A$  is the reduced density matrix over the subsystem  $A$ , found by taking the partial trace over the  $B$  subsystem with bases  $|j\rangle_B$ :

$$\rho_A = \text{Tr}_B[\rho] = \sum_j (I_A \otimes \langle j|_B) \rho (I_A \otimes |j\rangle_B) \quad (3.5)$$

Rényi entropies were introduced in [44] as a generalisation of Shannon entropies. Whilst Rényi entropies capture meaningful quantum correlations, they do not satisfy the useful subadditivity condition:

$$S(\rho_{A \cup B}) \leq S(\rho_A) + S(\rho_B) \quad (3.6)$$

For bipartite systems  $A \cup B$ . Fortunately, taking the limit  $n \rightarrow 1$  we recover the von Neumann entanglement entropy:

$$S(\rho) = -\text{Tr}(\rho \log \rho) \quad (3.7)$$

which is subadditive [45]. Note that all Rényi entropies are symmetric with respect to the subsystem, i.e.  $S_n(\rho_A) = S_n(\rho_B)$  [4], which also suggests that an area law would be reasonable to expect: if  $|A| > |B|$ , it would be odd for  $S(\rho_A) = S(\rho_B)$  if entropy scaled with volume.

Unfortunately, the entanglement entropy is only measurable if the system is in a pure state and if it is bipartite [4]. The only other measurable form of entanglement is the *negativity*. Before defining negativity, it is useful to define the *partial trace*:

$$\langle \varphi_A \varphi_B | \rho_A^{T_2} | \varphi'_A \varphi'_B \rangle \equiv \langle \varphi_A \varphi'_B | \rho_A | \varphi'_A \varphi_B \rangle \quad (3.8)$$

where  $\{\varphi_X\}$  is a basis for subsystem  $X$  [1]. We also define the *trace distance* of  $A$ :

$$\|A\| = \text{Tr} \sqrt{AA^\dagger} \quad (3.9)$$

which in turns lets us define the negativity:

$$\mathcal{N}(\rho_A) = \frac{\|\rho_A^{T_2}\| - 1}{2} \quad (3.10)$$

Assuming  $A$  is Hermitian, the trace distance of  $A$  is sum of the absolute value of the eigenvalues of  $A$  [4]. Hence the negativity measures the ‘negativity’ of the eigenvalues of  $A$ . Given the discussion about the Peres criterion, it is clear that this quantity measures the negativity of the partially transposed density matrix. Whilst this is monotone [46], it is not additive under the tensor product. However, we can take the logarithmic negativity:

$$\varepsilon(\rho_A) = \ln \|\rho_A^{T_2}\| \quad (3.11)$$

which is suitable additive. In this report we will compute the entanglement entropy and the entanglement negativity for a variety of systems, both analytically and with numerical methods. In the following section we will outline the principle model that we study as well as the SDRG procedure.

## 4 The Random Inhomogeneous Chain and the SDRG method

### 4.1 Random Inhomogeneous 1D Chain

The random inhomogeneous spin- $\frac{1}{2}$   $XXZ$  chain with  $L$  spins and open boundary conditions (OBC) has the Hamiltonian:

$$H = \sum_{i=1}^{L-1} J_i \left( S_i^x S_{i+1}^x + S_i^y S_{i+1}^y + \Delta S_i^z S_{i+1}^z \right) \quad (4.1)$$

$S_i^x$  is a spin component  $x$  operator acting on site  $i$ ,  $J_i$  is a random coupling connecting site  $i$  to  $i + 1$ , and  $\Delta$  is an anisotropy parameter. For periodic boundary conditions (PBC) and additional term for  $i = L$  is needed. With  $\Delta$  being non-zero we have the  $XXY$  random chain and with  $\Delta = 0$  we have the  $XX$  chain. With the  $XX$  chain the model is analytically solvable [21].

More details of how the couplings  $\{J_i\}$  are calculated for the in will be given in more detail in the relevant sections. For now it is sufficient to explain the principle disordered contribution to the random couplings, namely the probability distribution:

$$P_\delta(J) \equiv \delta^{-1} J^{-1+1/\delta} \quad (4.2)$$

Clearly as  $\delta \rightarrow 0$  the disordered contributions tend to 1 and we recover the clean spin chain. For  $\delta \rightarrow 1$  we approach a uniform distribution on  $[0, 1]$ . As  $\delta \rightarrow \infty$  we approach the infinite randomness fixed point (IRFP), which describes the asymptotic state of the distribution of  $\{J_i\}$  under successive SDRG steps (see 4.3) [13].

### 4.2 SDRG Procedure

We will summarise the SDRG procedure for the inhomogeneous 1D spin chain following [1]. To begin with, we identify the strongest coupling  $J_M$  and consider the energy of this interaction  $\mathcal{H}_0$ :

$$H_0 = J_M \vec{S}_l \cdot \vec{S}_r \quad (4.3)$$

The groundstate of this microsystem is

$$|s\rangle \equiv 2^{-1/2} (|\uparrow_l \downarrow_r\rangle - |\downarrow_l \uparrow_r\rangle) \quad (4.4)$$

Treating this as a perturbation, we can calculate a new effective coupling between the spins  $l - 1$  and  $r + 1$ <sup>2</sup>:

$$J' = \frac{J_l J_r}{(1 + \Delta) J_M} \quad (4.5)$$

Repeating this process identifies a *flow* of couplings from one step to the next:

$$(\cdots, J_l, J_M, J_r, \cdots)_L \rightarrow \left( \cdots, \frac{J_l J_r}{(1 + \Delta) J_M}, \cdots \right)_{L-2} \quad (4.6)$$

Importantly, given that  $J_M > J_{(l/r)}$ , the new coupling  $J'$  is smaller than either and the energy scale of the model is lowered.

### 4.3 SDRG Flow

The resulting distribution of couplings in terms of the SDRG step  $m$  can be given quantitatively, following [13]. We introduce logarithmic variables:

$$\beta_i^{(m)} \equiv \ln \frac{J_M^{(m)}}{J_i^{(m)}}, \quad \Gamma^{(m)} \equiv \ln \frac{J_M^{(0)}}{J_M^{(m)}} \quad (4.7)$$

---

<sup>2</sup>Details of the perturbation calculations can be found in [1] as well.

where  $J_M^{(m)}$  is the strongest coupling at the SDRG step  $m$ . The flow equation to be solved is given by [13] as:

$$\frac{dP}{d\Gamma} = \frac{\partial P(\beta)}{\partial \beta} P(0) \times \int_0^\infty d\beta_1 \int_0^\infty d\beta_2 \delta(\beta - \beta_1 - \beta_2) P(\beta_1) P(\beta_2) \quad (4.8)$$

which is solved with the ansatz:

$$P^*(\beta) = \frac{1}{\Gamma} \exp\left(-\frac{\beta}{\Gamma}\right) \quad (4.9)$$

Equation 4.8 is an attractor for *any* initial distribution of the couplings, not just the distribution described in equation 4.2.

As an initial test of the SDRG procedure we implemented, we have tracked the flow of the logarithmic couplings in figure 4.1. This is a close reproduction of a similar figure in [1] and shows that the SDRG process is indeed working correctly.

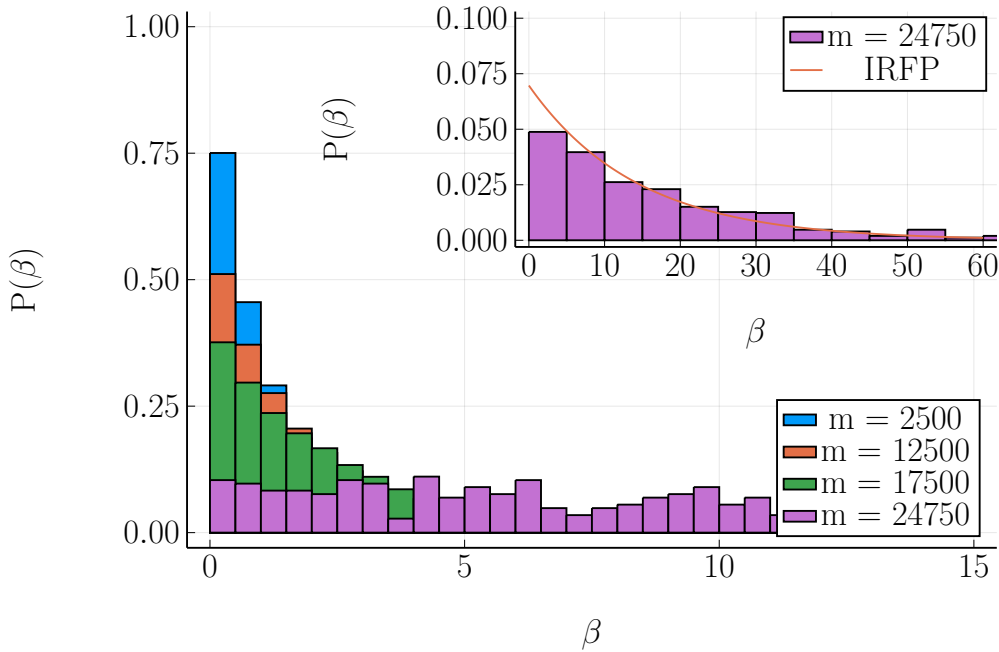


Figure 4.1: SDRG flow for  $L = 50,000$  spins in the disordered XXY chain ( $\Delta = 1$ ) where  $\delta = 1$ . The main plots shows the  $\beta$  distribution of the remaining bonds at the  $m^{\text{th}}$  step of the SDRG process. The inset plot shows subset of the  $\beta$  distribution late into the SDRG process with the IRFP line overlaid. The data is an excellent fit to the analytical prediction.

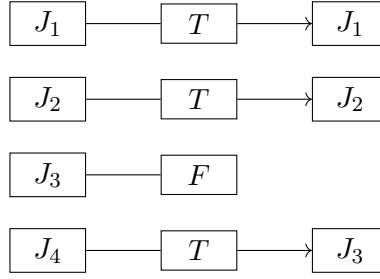


Figure 5.1: Diagram of the data masking procedure used to iteratively eliminate the bonds from data vector. The approach is size stable so minimises the need for allocations during the procedure.

## 5 Algorithmic Implementation and Complexity

We will briefly detail the main SDRG algorithm we have implemented for this report. Where necessary, we will add more details about how analyses were implemented as we reach them.

In studying disordered systems, we frequently need to take averages over disorder, i.e. many different realisations of the system in question. In many cases the number of trials must be very large for the required observables to converge - see [47] and [1] for examples of these issues. Thus an efficient and reliable algorithm is essential.

The key feature of our SDRG implementation is that it is almost totally memory static - that is, little or no extra memory is allocated in the computer every time a new disorder realisation is run. Rather, the existing memory used to hold data (e.g. bond strengths) is updated at the start of each realisation, and during the elimination process a ‘mask’ vector is maintained that tracks which bonds are active and should be used in calculation. The one off allocation of this mask vector is computationally very cheap compared to continually reallocating previous memory. An illustration of this approach can be seen in figure 5.1 and a psuedo-code version of our implementation can be seen in table 1.

---

### Algorithm 1: SDRG step algorithm

---

**Data:**  $\{J\}, L, \{(s_1, s_2)\}$   
**Result:**  $\{(s_1, s_2)\}$   
 $m \leftarrow 1$ ;  
 $active \leftarrow \{T\}^L$ ;  
 $n\_active = sum(active)$ ;  
**while**  $n\_active > 2$  **do**  
     $J_M \leftarrow max\{J_i\}$ ;  
     $J_l \leftarrow J_{M-1}$ ;  
     $J_r \leftarrow J_{M+1}$ ;  
     $J' \leftarrow \frac{J_l J_r}{(1+\Delta)J_M}$ ;  
     $active_M \leftarrow F$ ;  
     $active_{M+1} \leftarrow F$ ;  
     $\{(s_1, s_2)\}_m \leftarrow \{(M, M+1)\}$ ;  
     $m += 1$ ;  
     $n\_active = sum(active)$ ;  
**end**  
 $\{(s_1, s_2)\}_{L \div 2} \leftarrow \{(J_1, J_2)\}$ ;  
**return**  $\{(s_1, s_2)\}$ ;

---

To given an estimate of the efficiency of this procedure, we benchmarked the code for varying levels of machine precision and vary system lengths  $L$ . The results can be seen in figure 5.2. The elimination procedure for a system of  $L = 1000$  spins is on the order of four microseconds. This implies that upwards of 200,000 SDRG eliminations can be calculated in one second.

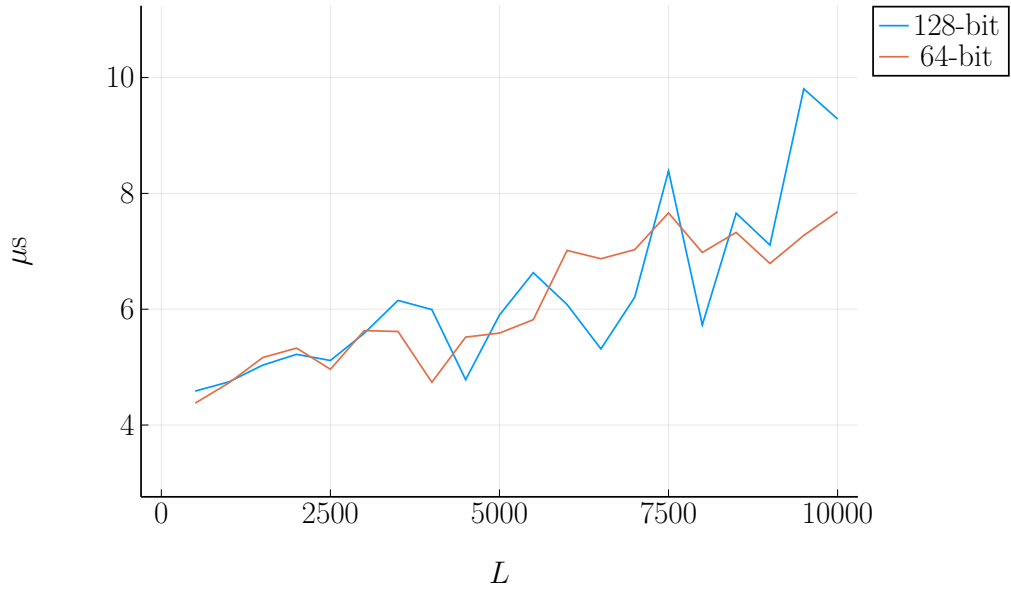


Figure 5.2: Benchmark results for our SDRG procedure. On the horizontal axis we measures the system length  $L$ , and on the vertical we report the median execution time for the complete SDRG procedure in microseconds. The execution time increases linearly in the system length for systems  $L$  in the order of thousands, and there is only a small performance penalty for using quadruple precision floating point numbers (i.e. 128 bits).

## 6 Existing Results and Verification

A number of results for the scaling of entanglement measures already exist (see [1], [2]). In this section we will reproduce these results and in the process, verify that the SDRG algorithm and related code works as expected.

### 6.1 Entanglement Entropy

As per [1], we measure the entanglement entropy of the disordered chain with and without periodic boundary conditions. The results are shown in figure 6.1. In this simulation we measure the entanglement entropy of a subsystem of length  $l$  located in the left hand side of the the XXY chain (i.e.  $\Delta = 1$ ). The position in the chain is not as relevant as it is in the later models where a strong spatial inhomogeneity is introduced, because the non-locality is much weaker and is not focused around a particular point (e.g. the centre).

For each simulation, we draw  $L$  random couplings from the uniform distribution over  $[0, 1]$  and run the SDRG algorithm (see 1). The SDRG algorithm returns a vector of tuples of sites, where each tuple represents a pair of spins. It is known from [7] that the ground state of the random spin chain (equation 4.1) is a *random singlet phase* (RSP), made up of  $L \div 2$  singlets each entangled in a valence bond, e.g. a valence bond state. Each pair of singlets has the state given in equation 4.4. On this vector of singlet pairs we then run the relevant analysis. In the case of this entropy calculation, for every realisation of the the RSP we measure the entanglement entropy (equation 3.7) for all window sizes  $l$ , and maintain a running mean of the result as a function of  $l$ . The entanglement entropy is calculated by dividing the system into the subsystem  $A$  and its complement  $A'$ : the entropy is the number of singlets links between these two subsections multiplied by  $\ln 2$ .

We run the analysis for  $L = 1000$  and  $L = 2000$  for 50,000 disorder realisations and in each case calculate from  $l = 10$  to  $l = L \div 2$  with an interval of 10 in between. For the periodic case (figures 6.1a and 6.1c) the finite size effects are smaller, and can be easily corrected with the following two mappings:

$$\ell \rightarrow L_c \equiv \frac{L}{\pi} Y\left(\frac{\pi \ell}{L}\right) \quad (6.1)$$

$$Y(x) = \sin(x) \left(1 + \frac{4}{3} k_1 \sin^2(x)\right) \quad (6.2)$$

where  $k_1 = 0.115$ , given by [48]. For the open case (figures 6.1b and 6.1d) the need is especially acute.

As can be seen in all four subfigures of figure 6.1, entropy scales logarithmically with the subsystem size. This is clearly an area law violation, and perfectly follows the prediction in [7]:

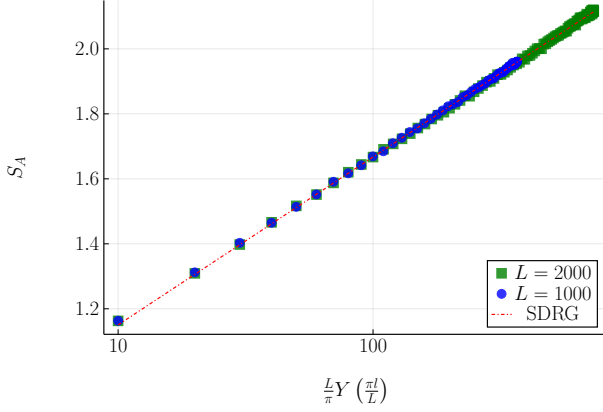
$$S_A = \frac{\ln 2}{3} \ln \ell + K \quad (6.3)$$

It should be noted that figures 6.1c the degree of divergence from the log-linear trend is less than is seen in [1]. This is because we have chosen to calculate the entanglement entropy only up to  $L \div 2$  as beyond half the chain, finite size effects will emerge even for the periodic implementation.

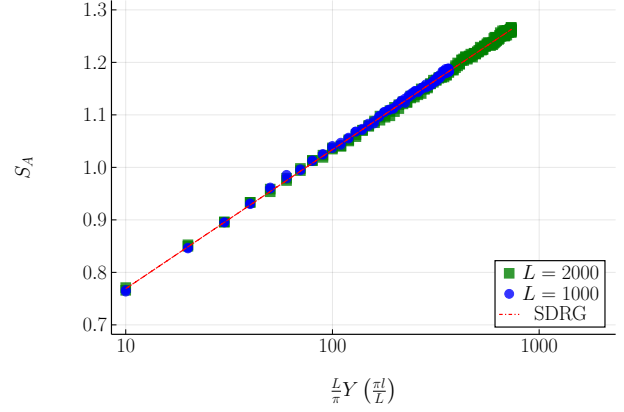
### 6.2 Logarithmic Negativity

In this section we recalculate the logarithmic negativity spectrum as reported in [1]. As we discussed in section 3, logarithmic negativity is in some sense a superior measure to the entanglement entropy because it is only measurable for pure states. As in [1], we calculate the logarithmic negativity of the one dimensional XXY chain (the same as in section 6.1). The pair of subsystems of length  $l$  is taken from the left hand side of the chain and extended in increments of 10 for every disorder realisation. The simulations are for the adjoint case, i.e.  $r = 0$  in [1]'s notation.

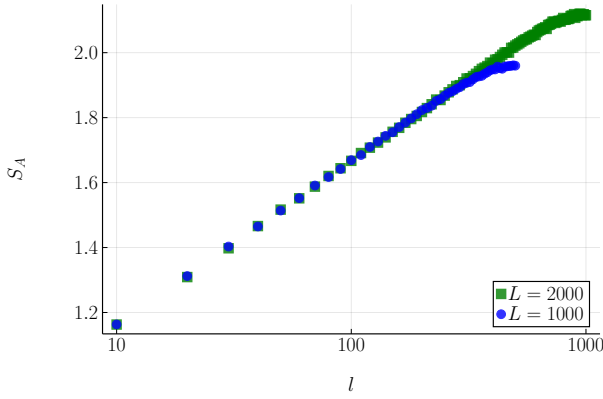
For the logarithmic negativity, we only need to measure the number of singlets shared between the two subsystems in  $A = A_1 \cup A_2$ , and multiply that by  $\ln 2$ . We run this analysis on systems of



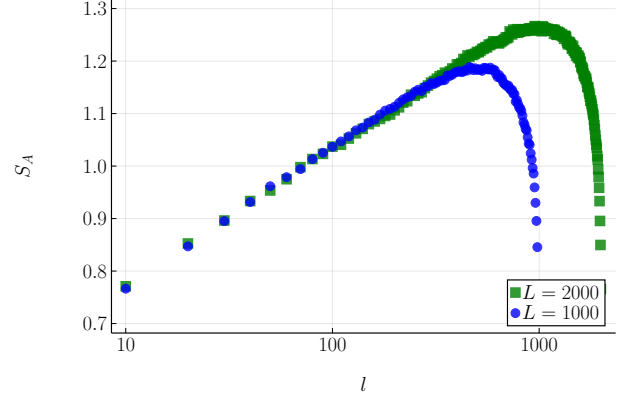
(a) Entanglement entropy of the  $XXY$  chain,  $\Delta = 1$ , adjusted  $l$ , PBC



(b) Entanglement entropy of the  $XXY$  chain,  $\Delta = 1$ , adjusted  $l$ , OBC



(c) Entanglement entropy of the  $XXY$  chain,  $\Delta = 1$ , no  $l$  adjustment, PBC



(d) Entanglement entropy of the  $XXY$  chain,  $\Delta = 1$ , no  $l$  adjustment, OBC

Figure 6.1: Entanglement entropy, recalculated from [1]. In all figures, we measure the entanglement entropy of a subsystem of length  $l$  located in the left hand side of the the  $XXY$  chain ( $\Delta = 1$ ). Each simulation is run for 50,000 trials. For implementation details, see 6.1. 6.1a: entanglement entropy of the periodic chain with the adjusted subsystem length  $L_c$ . 6.1b: entanglement entropy of the open chain with the adjusted subsystem length  $L_c$ . 6.1c: entanglement entropy of the periodic chain with the unadjusted subsystem length  $l$ . 6.1d: entanglement entropy of the open chain with the unadjusted subsystem length  $l$ .

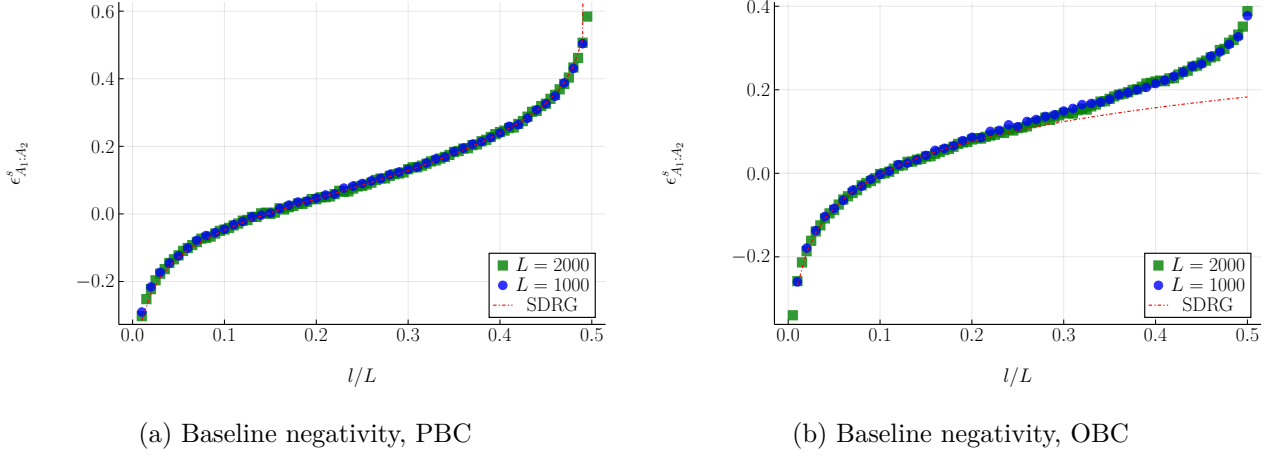


Figure 6.2: Shifted logarithmic negativity, recalculated from [1]. In all figures, we measure the logarithmic negativity of two adjacent subsystems of length  $l$  located in the left hand side of the the XXY chain (i.e.  $\Delta = 1$ ). Each simulation is run for 50,000 trials. For implementation details, see 6.2. 6.2a: shifted logarithmic negativity of the periodic chain with the subsystem length  $l$ . The fit is with equation 6.4. 6.2b: shifted logarithmic negativity of the open chain with the subsystem length  $l$ . The fit is with equation 6.5.

$L = 1000$  and  $L = 2000$  for 50,000 trials, as per the entanglement entropy calculations. We conducted the analysis in the OBC and PBC cases. The results can be seen in figure 6.2. In particular we have plotted the shifted negativity as defined in [1]:

$$\mathcal{E}_{A_1:A_2}^s = \mathcal{E}_{A_1:A_2} - \frac{\ln 2}{6} \ln L \quad (6.4)$$

Which is a perfect fit for the periodic chain (figure 6.2a). For the open chain, we use the following identity from [1] for the logarithmic negativity in the case of an infinite chain:

$$\mathcal{E}_{A_1:A_2} = \frac{\ln 2}{6} \ln \left( \frac{\ell_1 \ell_2}{\ell_1 + \ell_2} \right) + k, \quad (6.5)$$

which is a good fit for  $\ell/L \ll 1$ .

In both cases (entanglement entropy and logarithmic negativity), it can be seen that the entanglement scales with a logarithmic correction to the area law.

### 6.3 Randbow Chain

In this section we move on to reproducing the results of [2], which involves the modifying the couplings of the random chain to include an exponentially decaying term:

$$J_i \equiv K_i \times \begin{cases} e^{-h/2}, & i = 0 \\ e^{-h|i|}, & |i| > 0 \end{cases} \quad (6.6)$$

where the  $K_i$  terms are randomly distributed coefficients as before. This is known as the ‘randbow chain’. The significance of these random couplings is to enforce a *rainbow* phase if the exponential parameter  $h$  is strong enough [9] - see figure 6.3 for an illustration.

For the  $h \rightarrow \infty$  limit, the entanglement entropy of a subsystem  $A$  starting in the centre of the randbow chain (properly called the rainbow chain in this phase) scales as a volume law. This is because for any subsystem  $l$ , the subsystem of size  $l+1$  must contain another singlet link. For example, looking at figure 6.3, if our subsystem  $A$  starts as  $A = \{J_1\}$ , and then we extend it to  $A = \{J_1, J_2\}$ , these two subsystems have 1 and 2 singlet links in them respectively, and this holds for every other subsystem up to the maximum for  $l = L \div 2$ . Note that if we position the subsystem centrally in the chain, then the entanglement entropy is always zero for the strong  $h$  phase as we only have ‘complete singlets’ in our subsystem (see [9] for an illustration, figure 2(b)).



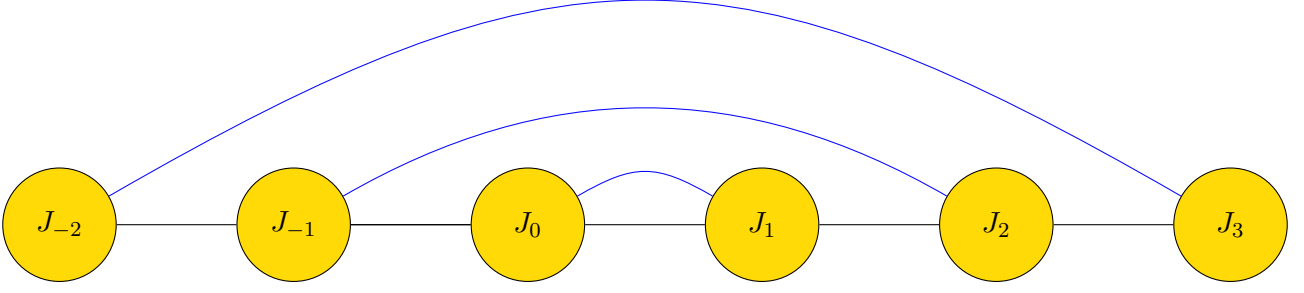


Figure 6.3: A rainbow chain as introduced in [9] and [2]. The central coupling  $J_0$  is by definition the strongest coupling for the clean chain or for sufficiently large  $h$ , so it will always be eliminated first. The black edges represent the couplings  $\{J_i\}$ , whereas the blue edges represent the singlet links. Note that for the rainbow chain to make sense, we must have an odd number of links and an even number of spins in the open chain, hence the asymmetry in the diagram.

For the  $h = 0$  phase we recover the random chain and the results from section 6.1 hold. However, for intermediate  $h$  we observe a square root correction to the area law (originally reported in [2]). This is presented in figures 6.4 and 6.5. As  $h$  increases, the scaling of the entropy gets closer and closer volume law phase, as the effect of the ‘rainbow’ dominates. As we approach  $h = 0$ , the effect is weaker and we approach the random phase again. In 6.4 we measure the scaling of the entanglement entropy for a subsystem  $A$  of length  $l$  with its left edge on the centre of the chain. This positioning guarantees that we capture the volume scaling as  $h$  increases. We run both experiments for 50,000 disorder realisations for the non-interacting open  $XX$  chain.

When we measure the entropy scaling for set ratios of  $h/\delta$ , we observe a data collapse as first reported in [2]. This is interestingly only the case of the SDRG procedure and does not hold in the exact solution for the  $XX$  chain (see section 6.5).

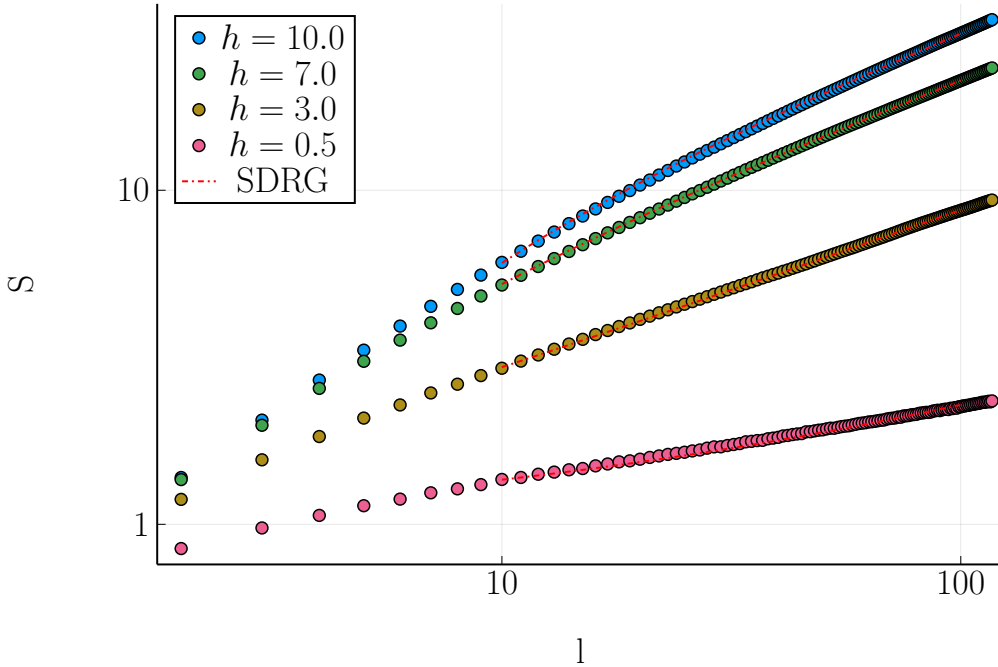


Figure 6.4: Scaling of the entanglement entropy for the open  $XX$  rainbow chain whilst varying the exponential parameter  $h$ . Notice the log-log scaling on each axis. Each experiment is run for 50,000 realisations of the disorder, and we measure the entanglement entropy of a subsystem  $A$  starting at the chain centre (offset by one to ensure the proper scaling) for each realisation. A fitted function of the form  $y = a + b\sqrt{x}$  is overlaid for each value of  $h$ .

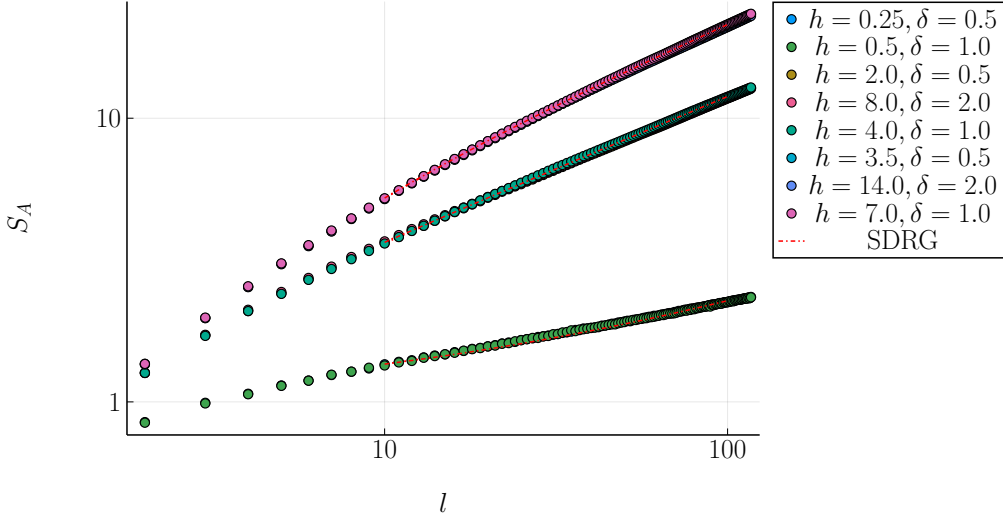


Figure 6.5: Scaling of the entanglement entropy for the open  $XX$  random chain whilst varying the exponential parameter  $h$  and the disorder parameter  $\delta$  in fixed ratios. Again, notice the log-log scaling on each axis. Each experiment is run for 50,000 realisations of the disorder, and we measure the entanglement entropy of a subsystem  $A$  starting at the chain centre (offset by one to ensure the proper scaling) for each realisation. A fitted function of the form  $y = a + b\sqrt{x}$  is overlayed for each value of  $h/\delta$ .

#### 6.4 Random Subregion Analysis

To further verify the findings of [2] and to verify our own SDRG implementation, we recalculated specific elements of the contour analysis performed in that paper. Specifically, to understand the square root scaling we consider the probability densities of the sizes of the rainbow and ‘bubble’ regions. In any given realisation of the random chain, there will be subregions of continuous rainbow links and regions of continuous ‘bubbles’ (see figure 6.6 for an example).

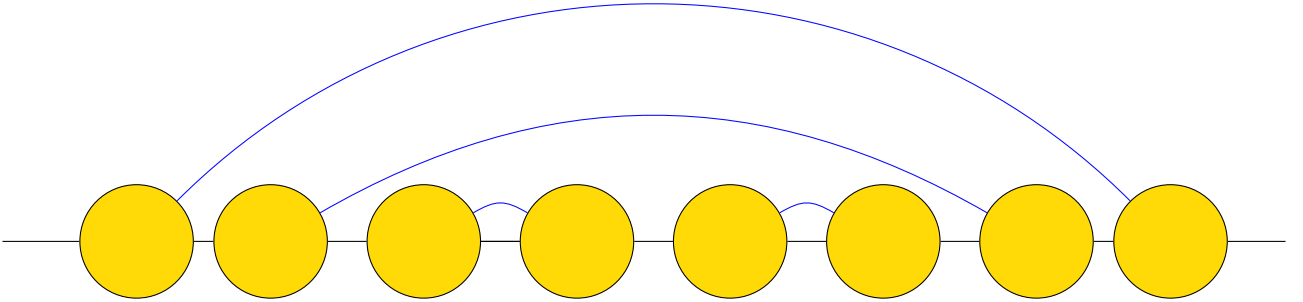


Figure 6.6: A demonstration of the bubble and rainbow subregions as named in [2]. The first two spins represent a rainbow region of  $l = 2$ , and the second four spins represent a bubble region of  $l = 4$ .

We denote  $P_r(l)$  the probability mass of seeing a rainbow subregion of length  $l$ , and similarly  $P_b(l)$  for the probability of a bubble subregion of length  $l$ . We report these probability mass functions in figures 6.7 and 6.8 respectively, both with disorder parameter  $\delta = 1$  and for a system size  $L = 1000$  in the  $XX$  chain. We observe that for the rainbow distribution  $P_r$ , the probability of a region of length  $l$  decays exponentially in  $l$ , and that the rate of decay depends on  $h$ . However, for the  $P_b$  distribution, we observe a much slower power law decay, implying that there is no characteristic size of a bubble region, and furthermore that this does not depend on  $h$  at a scale visible on the plot.

This leads to an argument that the scaling of the entanglement entropy scales as a square root. We presented the following argument, adapted slightly from that given in [2]. Firstly, we observe from

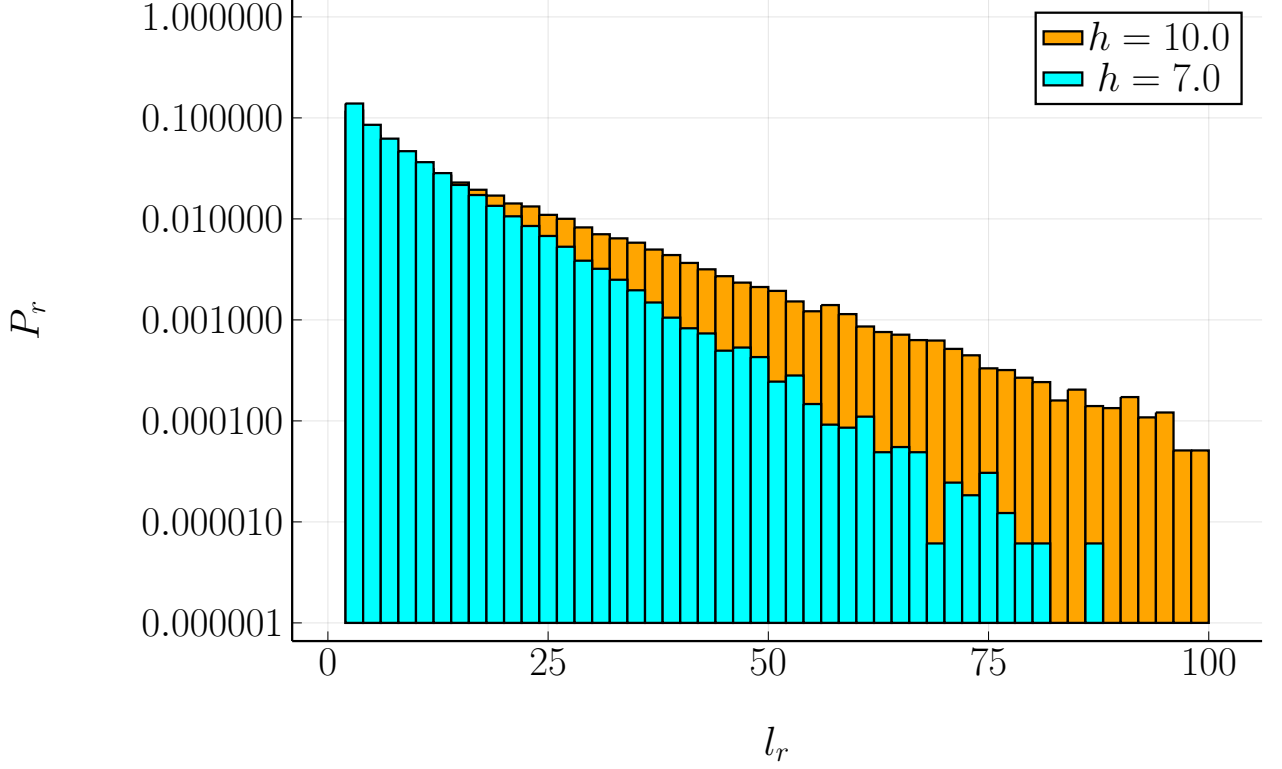


Figure 6.7: Probability density function  $P_r(l)$  of the lengths of rainbow subsystems. The data were collected by averaging over 10,000 disorder realisations for  $h = 10$  and  $h = 7$  in the open  $XX$  chain, solved with the SDRG method. Notice the logarithmic scale on the y-axis only, suggesting an exponential decay.

figure 6.8 that  $P_b(l) = l^{-3/2}$ , and thus:

$$\langle l_b \rangle = \int_2^l dl P_b(l) \propto l^{1/2} \quad (6.7)$$

Secondly, calling a ‘bubble region’ a subsystem of consecutive bubbles, and similarly a ‘rainbow region’, we notice that, very roughly, the number of bubble regions  $N_b$  must be equal to the number of rainbow regions  $N_r$ . Furthermore, dividing the total subsystem length  $l$  by the average length of a bubble region  $\langle l_b \rangle$  gives  $N_b$ , and thus:

$$\frac{l}{\langle l_b \rangle} \propto N_b = N_r \quad (6.8)$$

The entanglement entropy is equal to the number of rainbow links in the subsystem multiplied by  $\ln 2$ , which is equal to the number of rainbow regions multiplied by the average length of a rainbow region:

$$S_A \propto N_r \times \langle l_r \rangle \times \ln 2 \quad (6.9)$$

Bringing together equations 6.8 and 6.9, we get:

$$S_A \propto \frac{l}{\langle l_b \rangle} \times \langle l_r \rangle \times \ln 2 \propto l^{1/2} \langle l_r \rangle \ln 2 \quad (6.10)$$

which suggests the observed square root scaling.

## 6.5 Randbow Chain Exact Solution

Finally, we analyse the exact solution of the  $XX$  chain. This is done by forming a matrix  $C_{ij} = \langle c_i^\dagger c_j \rangle$  and taking a subset  $A$  of these matrix entries - this forms the partial density matrix with respect to the

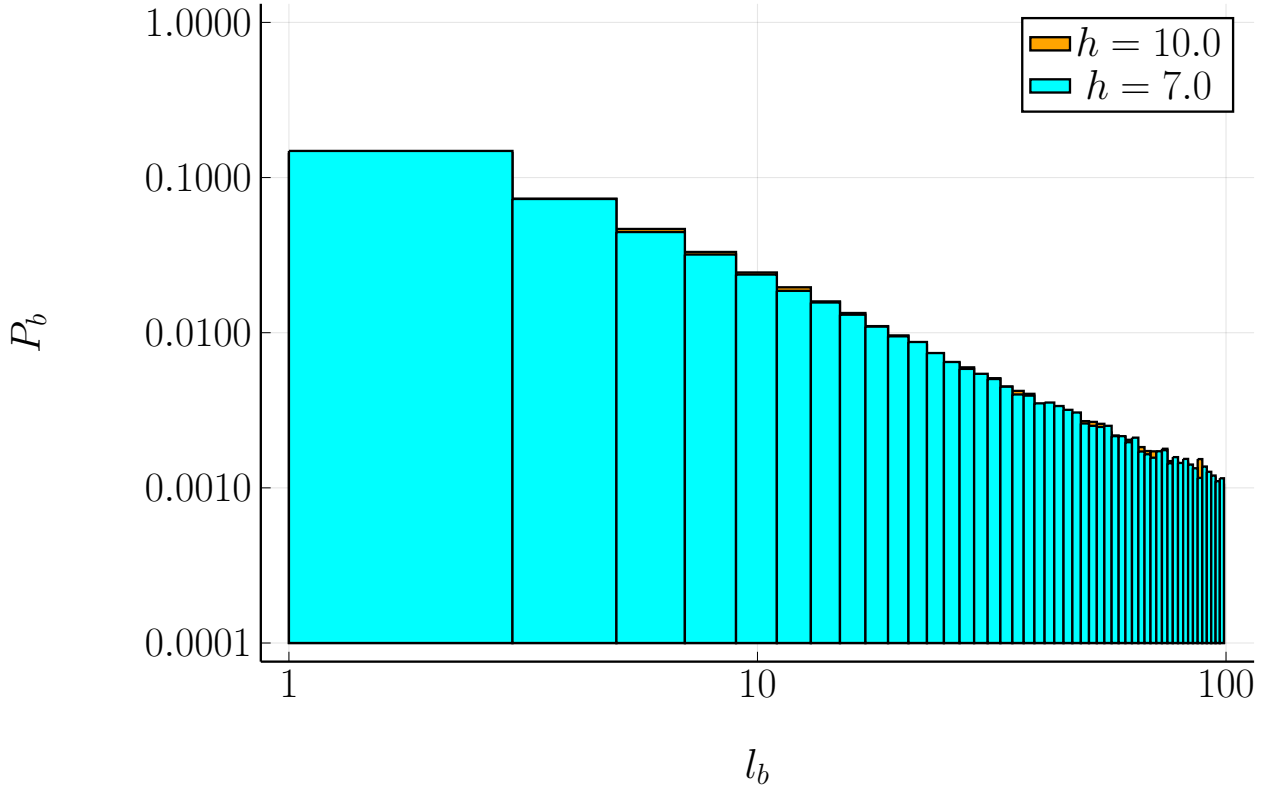


Figure 6.8: Probability density function  $P_b(l)$  of the lengths of bubble subsystems. The data were collected by averaging over 10,000 disorder realisations for  $h = 10$  and  $h = 7$  in the open  $XX$  chain, solved with the SDRG method. Notice the logarithmic scale on both axes, suggesting a power law decay.

A subsystem, from which we can calculate the entanglement entropy trivially. For a detail derivation, see appendix B.

In the following experiments, we calculate the exact solution to the  $XX$  random chain for a system with  $L = 100$  spins. We take an average over 1000 realisations of the disorder for each disordered system and calculate the entanglement entropy from  $l = 1$  to  $l = 32$  for each realisation. For accuracy these experiments were run with 128-bit floating point numbers, which slows down the computation significantly as most optimised linear algebra routines are designed for precisions of 64-bit or lower. The results for the disordered cases are shown in figure 6.9. Note the  $\log_2$  scaling on each axis. The entanglement entropy retains its square root scaling, but we observe that the data collapse onto the  $h/\delta$  ratios is no longer present. Furthermore, the absolute increase in  $h$  does increase the entanglement entropy at all scales  $l$ . This suggests that the SDRG procedure is not wholly accurate in the large  $l$  limit, perhaps because in the tail region of the spin couplings the values of  $J_i$  are so small that the second order perturbation used to develop the Dasgupta-Ma rule is no longer accurate.

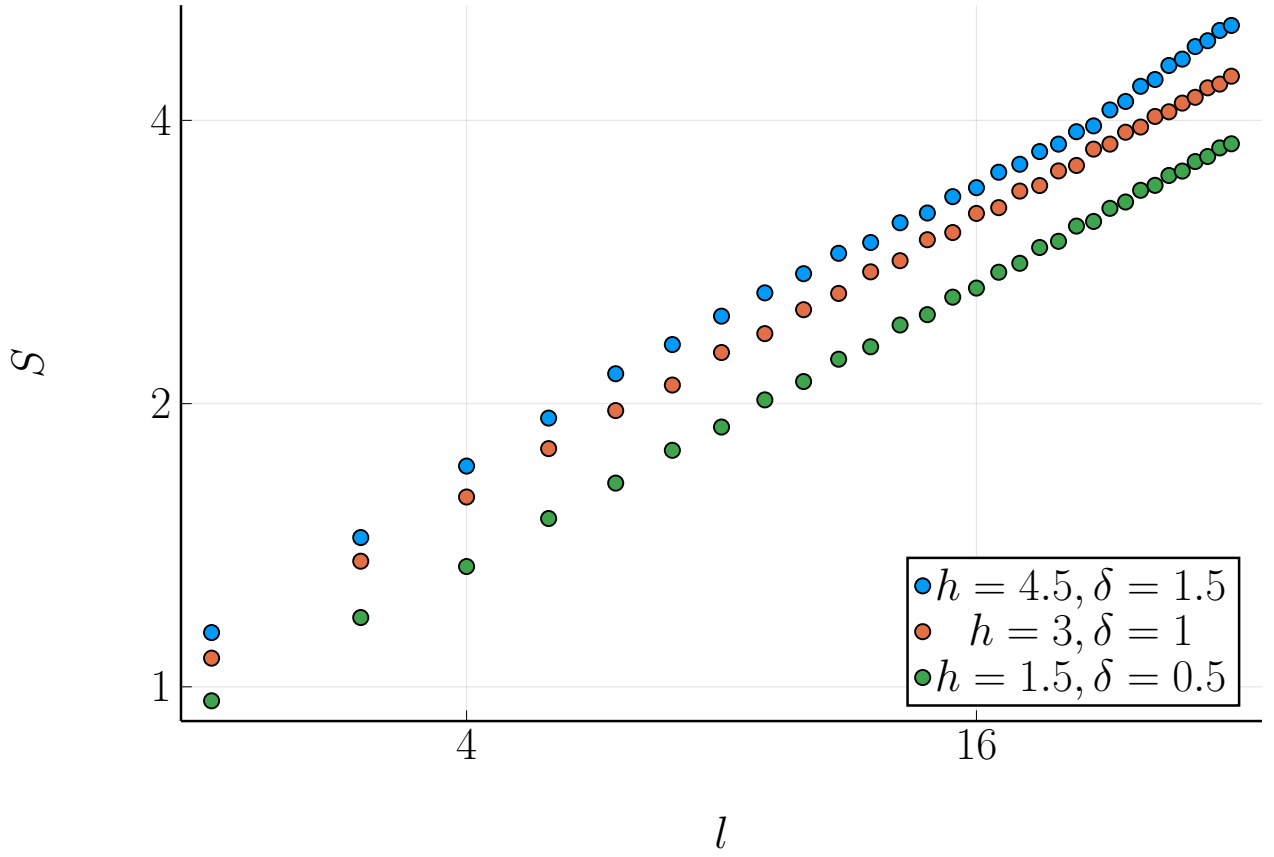


Figure 6.9: Entanglement entropy scaling of the  $XX$  random chain with the exact solution. We calculate the solution for the  $L = 100$  chain with  $\delta = 1$  for 1,000 disorder realisations. Notice the log-log scales. Notice that the data collapse on the ratio  $h/\delta$  is no longer present.

## 7 Entanglement negativity for the randbow chain

### 7.1 Analytical expectation

In the following sections, we begin our extension of the existing results. We start by analysing the logarithmic negativity we expect for an open randbow chain with two adjacent intervals as we vary the subsystem length  $l$ . This experimental setup is identical to that seen in 1.2, except that we use the randbow couplings rather than the basic disordered couplings.

For the  $h \rightarrow \infty$  limit, we would expect the negativity to follow the volume law. The argument is essentially the same as that made for the large  $h$  entanglement entropy: for every extra  $l + 1$ , we introduce another singlet link between  $A_1$  and  $A_2$ , thus we get a volume law.

For moderate values of  $h$ , we can predict a square root scaling via a very similar argument to that presented in 6.4. First, recall that the logarithmic negativity is simply the number of singlet links between the two subsystem, multiplied by  $\ln 2$ . Secondly, we assume that for moderate  $h$ , the groundstate of the SDRG procedure is symmetric with respect to the chain centre. This is reasonable for moderate  $h$  and is supported by further arguments with respect to the flow of eliminations presented in [2].

This allows us to consider just one of the two  $A$  subsystems (as we know that the other will be identical except for a reflection in the indices  $i$ ). Any rainbow links emerging from the subsystem  $A_2$  will be going to the subsystem  $A_1$  and vice versa<sup>3</sup>, and thus will contribute to the logarithmic negativity. To understand the scaling of the logarithmic negativity, then, we only need to understand the scaling of the entanglement entropy of the subsystem  $A_2$ , which we know to be a square root scaling.

It is important to point out that this argument, based on that given in [2], only holds in the non-interacting case. We will see in the numerical evidence that that is indeed the case and the interacting model shows a saturating behaviour that cannot yet be predicted analytically.

### 7.2 SDRG results

We measure the logarithmic negativity of two adjoint subsystems in the  $XX$  and  $XXY$  randbow chains, with  $L = 1000$  and  $2000$  in both cases. We use the SDRG procedure for 50,000 realisations of the disorder each, and plot the regular (i.e. not shifted as per 6.2) logarithmic negativity as a function of the adjusted subsystem length  $l/L$ . In both cases we use the parameters  $h = 1, \delta = 1$  for the moderate inhomogeneity regime. Our results are shown in figure 7.1.

As can be seen from figure 7.1a, in the  $XX$  case the square root scaling is captured perfectly. Furthermore, for larger values of  $l$  we notice that the logarithmic negativity is higher for a given fraction of the chain. This is to be expected: for a longer chain, there will be more singlet links in a subsystem for length  $0.5L$ , etc.

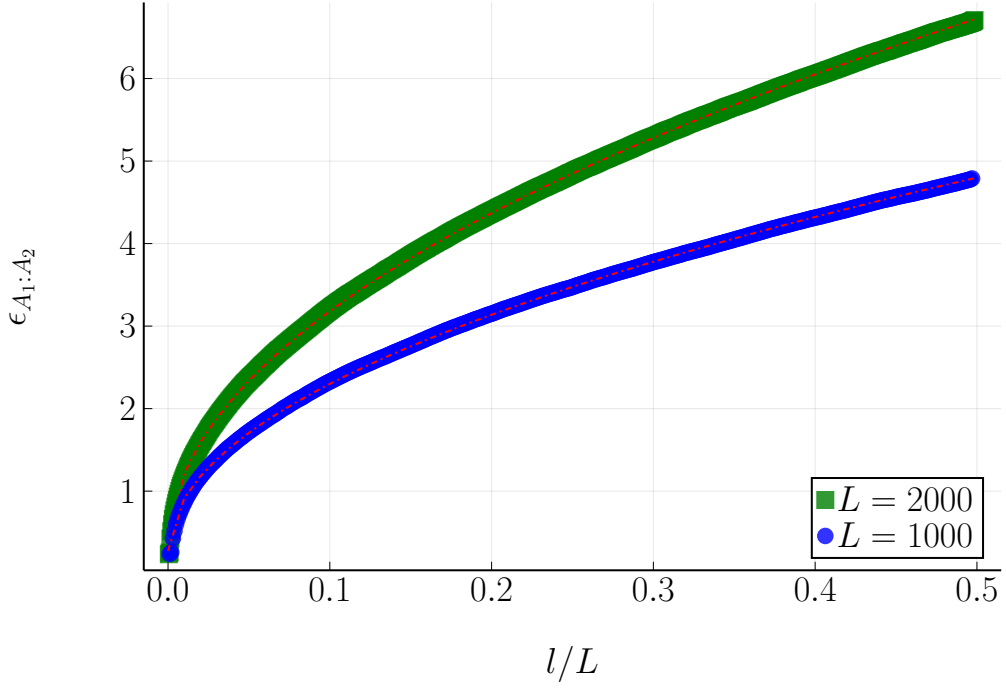
In the  $XXY$  model, we observe the same saturation behaviour reported for the entanglement entropy in [2]. This is to be expected given the the argument made above in section 7.1: to calculate the logarithmic negativity we only need to know the entanglement entropy, and we already expect this to saturate in  $l$ .

It is interesting to note that the saturation implies a return to the area law regime, and to consider why this occurs only in the interacting case. It is argued in [2] that the bubble regions in the interacting model are much more stable, which invalidates the heuristic argument presented for the square root scaling and leads to a saturation, because there is not enough space in the subsystem for rainbow links. The details of this argument are beyond the scope of this report but are covered in more detail in [2].

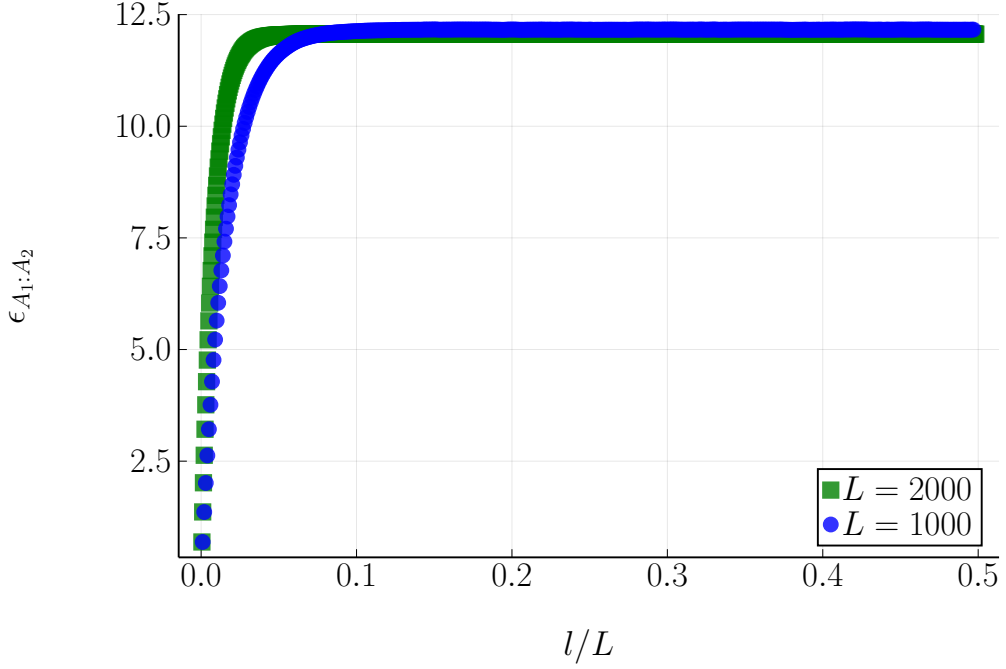
As an additional measure of the rate at which entanglement decays from the centre of the chain, where bonds are very strong, we measure the logarithmic negativity as we vary the interval  $r$  between two adjacent intervals in the  $XX$  and  $XXY$  chains. We consider only even  $r$ , with the interval spaced evenly over the centre of the chain (see figure 1.2 for a visualisation) with  $L = 1000$ . We observe that

---

<sup>3</sup>We ignore the possibility that a rainbow link could leave  $A_2$  ‘to the right’ and attach to the remainder of the chain. It is shown in [2] that this is a very accurate approximate from moderate  $h$ .



(a) Logarithmic negativity for the open random XX chain.



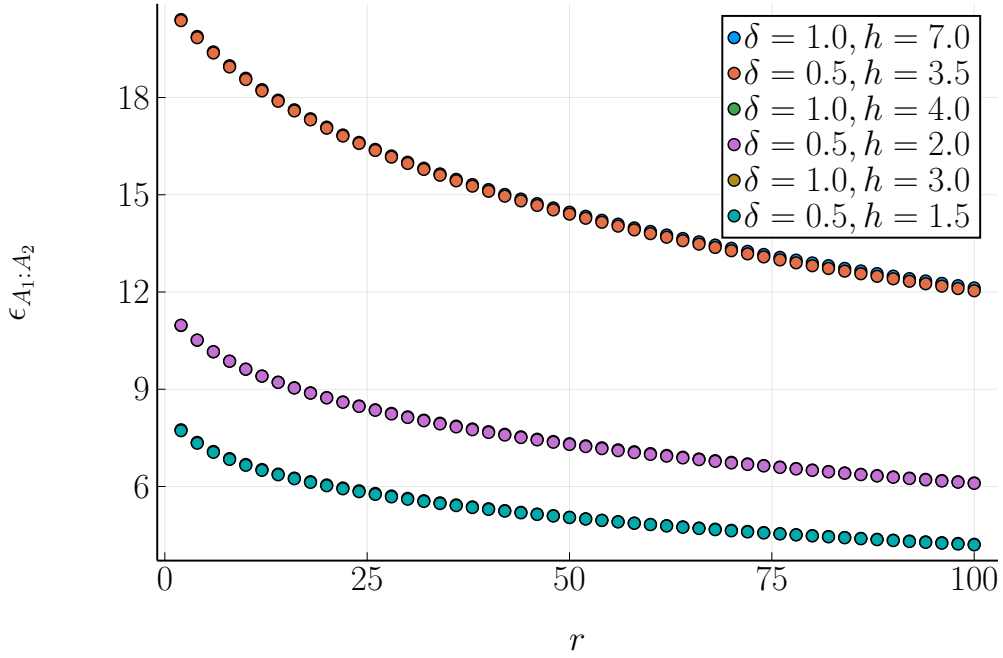
(b) Logarithmic negativity for the open random XXY chain.

Figure 7.1: Logarithmic negativity scaling in the open random chain for adjoint subsystems. We set  $h = 1, \delta = 1, L = 100$  in both figures and measure the logarithmic negativity over 50,000 disorder realisations. We place the subsystems  $A_1$  and  $A_2$  in the centre of the chain, i.e. with the right hand edge of  $A_1$  next to the left hand edge of  $A_2$ . In both figures we run the experiment for  $L = 1000$  and  $L = 2000$ . 7.1a: scaling in the  $XX$  regime. A square root scaling is observed, reflecting analytical expectations and the results from 6.5. 7.1b: scaling in the  $XXY$  regime,  $\Delta = 1$ . We observe that the logarithmic negativity saturates quickly in both system lengths.

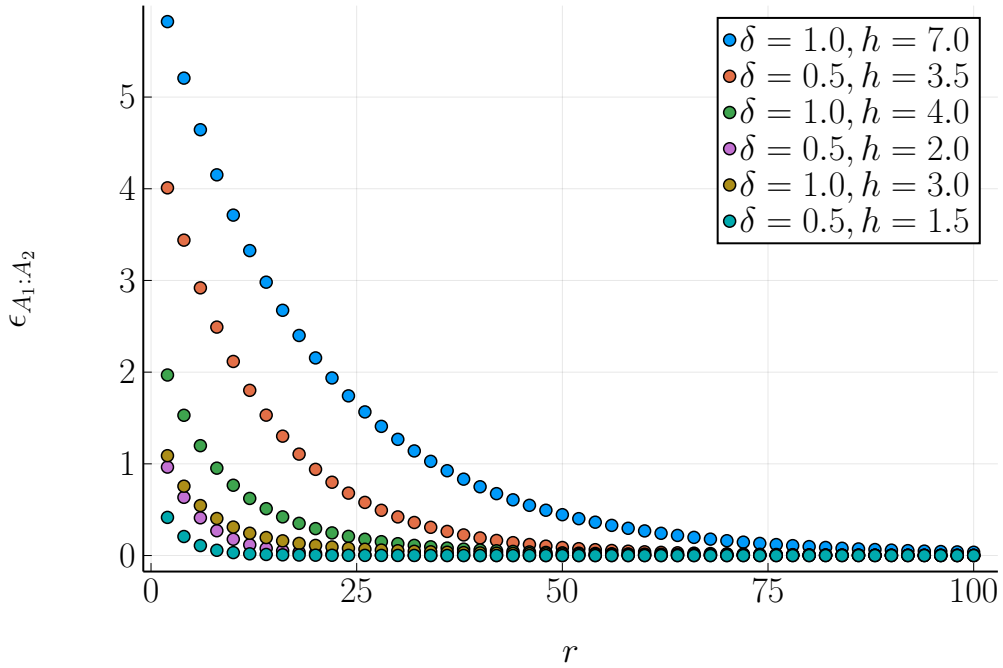
the in the  $XX$  case, the logarithmic negativity decays relatively slowly as  $r$  increases. This is to be expected given the previously discussed stability of the rainbow regions in the  $XX$  case relative to the bubble regions. Furthermore, we notice a strong data collapse onto the ratios  $h/\delta$ , just as for the previous measures of entanglement.

However, in the interacting  $XXY$  case, the logarithmic negativity decays far more quickly, as expected from the saturating behaviour we see in figure 7.1b. This is a corollary of figure 7.1b: as we extend further into the extremes of the chain, the entanglement is generally local and we lose long distance information.





(a) Random central negativity with varied  $r$ , XX, OBC



(b) Random central negativity with varied  $r$ , XX, OBC

Figure 7.2: Logarithmic negativity scaling in the open random chain for disjoint subsystems as we vary  $r$ . We measure the logarithmic negativity over 50,000 disorder realisations. We place the subsystems  $A_1$  and  $A_2$  in the centre of the chain separated by an even interval  $r$ , located in the centre of the chain.  $L = 1000$  and  $l = 100$  in both figures. 7.2a: the XX chain. The logarithmic negativity decays relatively slowly, in line with figure 7.1a. We also observe a strong data collapse onto the ratio  $h/\delta$ . 7.2b: scaling in the  $XXY$  regime,  $\Delta = 1$ . The logarithmic negativity decays much more quickly, in line with figure 7.1b, and there is no observable data collapse other than the  $r \rightarrow 0$  limit in which all entanglement is lost.

## 8 Power law systems

In [9], it is mentioned that the couplings must decay relatively quickly in order for the complete rainbow chain to be enforced. In particular they suggest that:

$$J_i = \epsilon^{\alpha(i)} \quad (8.1)$$

where  $\alpha(i)$  is monotonically decreasing<sup>4</sup>. To explore how sensitive the scaling of the rainbow and randbow phases is to the speed of this decay, we consider a new power-law system with couplings given by:

$$J_i \equiv K_i \times \begin{cases} 2, & i = 0 \\ |i|^{-\alpha}, & |i| > 0 \end{cases} \quad (8.2)$$

In the follow sections, we discuss the analytical expectations for the scaling of the entanglement entropy and the logarithmic negativity in the case of the power-law couplings.

### 8.1 Power law systems: analytical expectations

In [2], it is possible to derive analytical expectations for the randbow chain only in the strong inhomogeneous limit  $h \rightarrow \infty$  (see in particular section VI.A). This is because only in the inhomogeneous limit (and with symmetric  $J_i$ ) can we be sure the the central bond will always be eliminated first and that the elimination process will be symmetric with respect to the chain.

Unfortunately, for the power-law system, we cannot guarantee that the central bond will be eliminated first, nor that the process will be symmetric. The reason is that the effect of the power-law component is not enough, relative to the effect of the  $\mathcal{O}(1)$  disorder factor, to rapidly reduce the consecutive couplings. Given that, as discussed in section 4.2, the elimination rule always reduces the energy scale, the couplings around the elimination site must be small enough to still be smaller than the new  $J'$  coupling. In the power-law system, this can be guaranteed to be the case.

Therefore we cannot make any quantitative predictions about the scaling of the entanglement entropy or the logarithmic negativity for the power-law system. However, given that we do not expect the couplings to decay quickly enough to maintain a rainbow phase, we might expect that the power-law system will behave at least asymptotically as the simple disordered system. Thus we can make the following general hypotheses:

1. The entanglement entropy will scale in a manner similar to the simple disordered spin chain as seen in section 6.1.
2. The logarithmic negativity will also scale in a manner similar to the simple disordered spin chain as seen in section 6.2.

We will explore these results within the SDRG framework and with the exact solution.

### 8.2 Entanglement Entropy: SDRG and exact results

We start by calculating the scaling of the entanglement entropy of the open  $XX$  power-law chain with  $L = 1000$  and  $L = 2000$ . We use  $\delta = 1$  in all of our experiments and position the subsystem  $A$  with the left hand edge on the centre of the chain, the properly capture the scaling as in the randbow experiment (see 6.3). We run all of the experiments for 50,000 disorder realisations and the results are shown in figure 8.1.

In both figures, we can see that, as expected, the entanglement entropy scales similarly to the simple disordered model. For very low  $l$  we notice that the entanglement scales very quickly, which suggests that the rainbow phase does survive for at least the first few eliminations on average. After the initial phase, the scaling becomes quasi-logarithmic, confirming the hypothesis in section 8.1.

---

<sup>4</sup>In [9] they say ' $\alpha(i)$  is a function that is monotonically increasing' but this would not given the desired result, as couplings would increase exponentially from the chain centre!

Furthermore, we notice that for larger values of  $\alpha$ , the entanglement entropy is generally larger. This accords with our intuition that for stronger inhomogeneity, the rainbow regions should be more stable and they are the regions that contribute to the entanglement entropy. Lastly, we observe some finite size effects for  $l/L \approx 1/2$ . We have not attempted to fit any of the analytical curves from the simple disordered model due to the very different low  $l$  region.

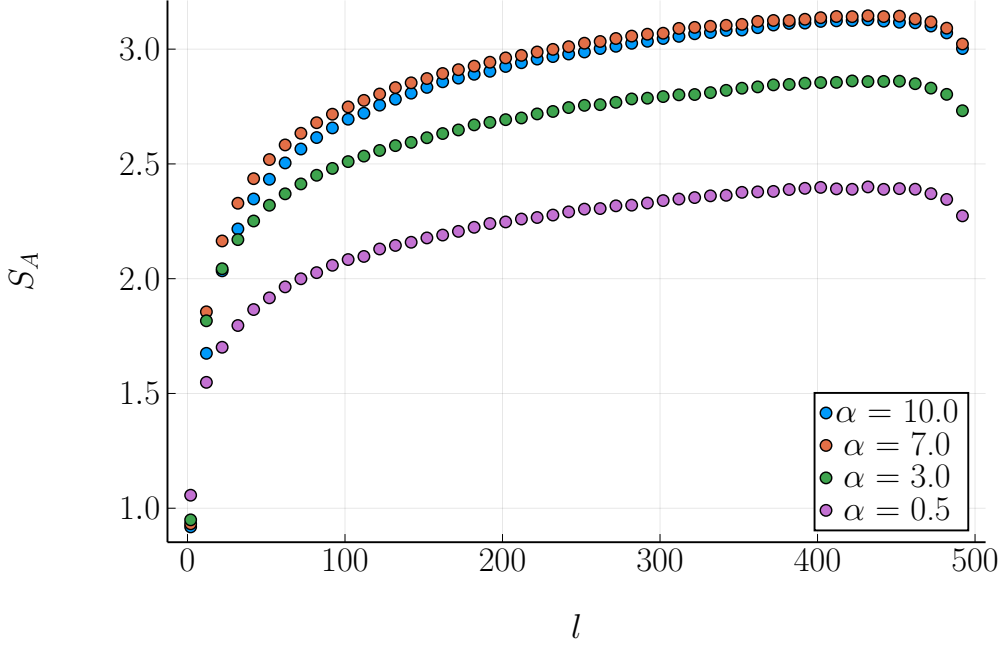
Furthermore, we measure the entanglement entropy via the exact solution, as we did for the randbow chain and as detailed in section B. Over 1000 disorder realisations, we measure the scaling of the entanglement entropy of the  $XX$  power-law chain for an open chain of length 100. Our results are shown in figure 8.2. Once again, the scaling of the entropy is logarithmic (notice the log-log scaling) and this matches the general scaling pattern observed in figures 8.1a and 8.1b. Interestingly, we observe a strong data collapse onto the ration  $\alpha/\delta$ , which accords with our intuition that the power-law system is qualitatively different to the randbow system, which did not show a data collapse in the exact solution.

### 8.3 Logarithmic negativity scaling

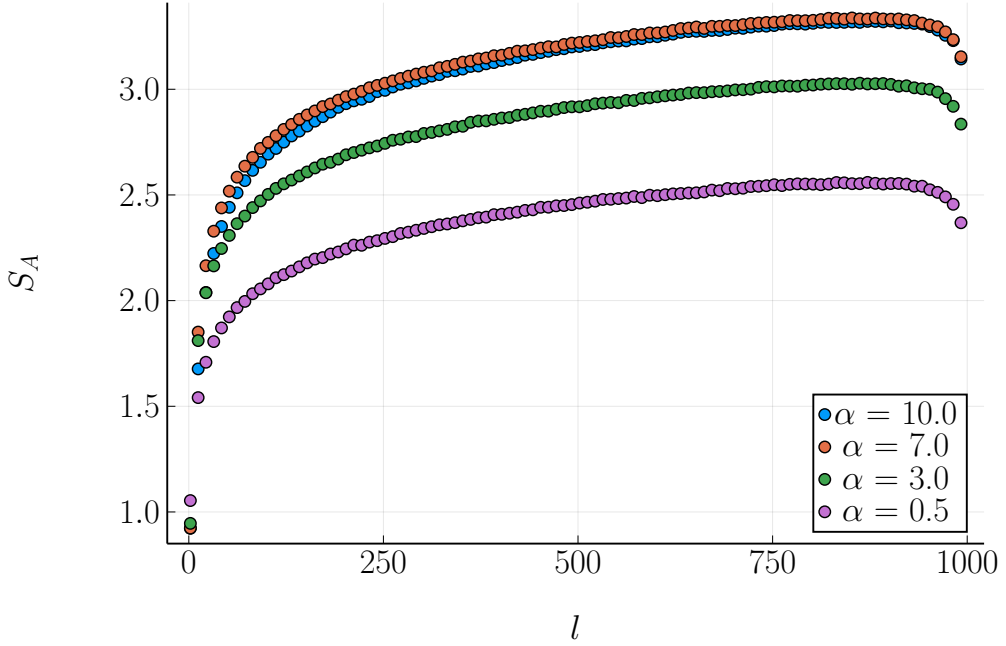
In this section, we look at the logarithmic negativity of the power-law system. Specifically we measure the logarithmic negativity of the open  $XX$  and  $XXY$  power-law chains for  $L = 1000$  and  $L = 2000$ . We run each experiment for 50,000 disorder realisations, and our results are shown in 8.3.

For both values of  $L$ , we observe that the scaling is identical to that of the simple disordered chain. This confirms our earlier hypotheis about the power-law systems. Interestingly, the curve for  $L = 2000$  is higher in both the  $XX$  and the  $XXY$  experiments than the  $L = 1000$  curve. This is best explained by the presence of some persistent rainbow regions even in the power-law model: in terms of absolute logarithmic negativity, half of the  $L = 2000$  rainbow chain will contain more singlet links between the two subsystems than the equivalent subsystem of a relative size for  $L = 1000$ .

Finally, we calculate the scaling of the logarithmic negativity for a varying interval  $r$  between two subsystems, in a manner identical to that discussed in 7.2. Our results for the open  $XX$  and  $XXY$  chains with disorder  $\delta = 1$  are reported in figure 8.4. We observe that, much like the interacting randbow chain, the logarithmic negativity decays much more quickly than in the randbow chain, which we would expected given the relative instability of the rainbow regions.



(a) Powerbow entropy via SDRG,  $L = 1000$ , varying  $\alpha$ , OBC



(b) Powerbow entropy via SDRG,  $L = 2000$ , varying  $\alpha$ , OBC

Figure 8.1: Entanglement entropy for the open  $XX$  power-law system, calculated via the SDRG method. We  $L = 1000$  and  $2000$ . In both figures, we calculated the entropy of a subsystem  $A$  with the left edge on the centre of the chain to capture the proper scaling over 50,000 disorder realisations. For each system size we ran the experiment with a different parameter  $\alpha$  as per equation 8.2. Figure 8.1a:  $L = 1000$ . Figure 8.1b:  $L = 2000$ .

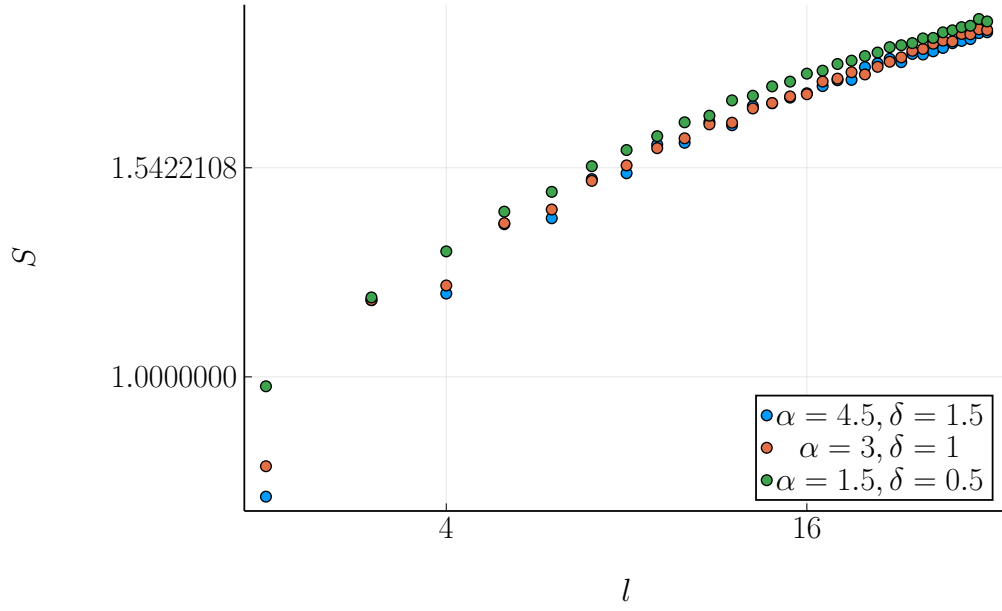
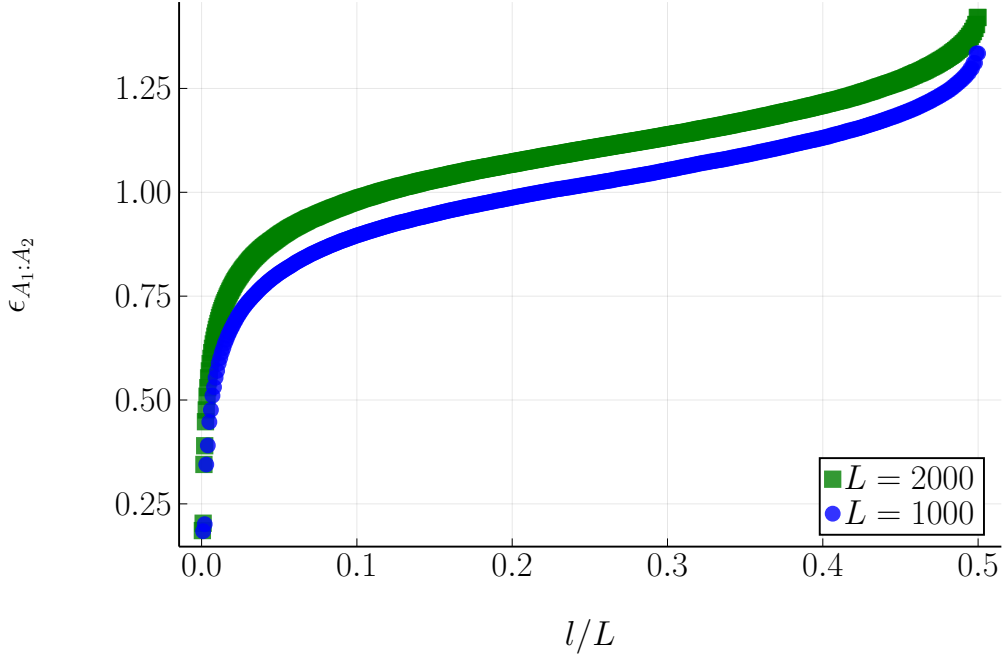
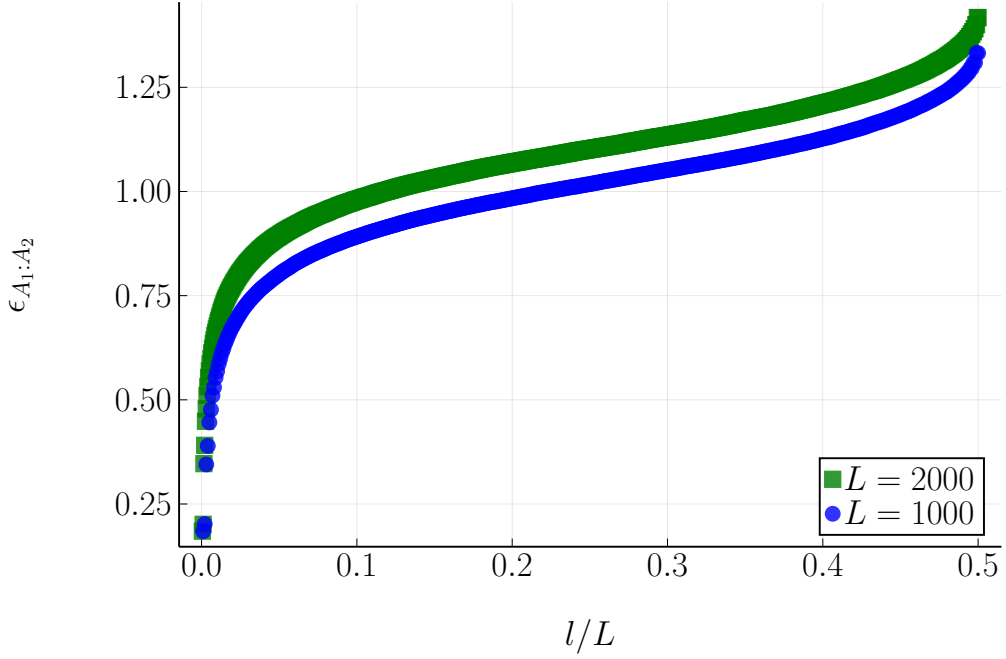


Figure 8.2: Entanglement entropy of the open  $XX$  power-law system, calculated with the exact solution over 1,000 disorder realisations with  $\delta = 1$ . For each experiment we vary the  $\alpha$ . The system length is  $L = 100$ . Notice the log-log scale.

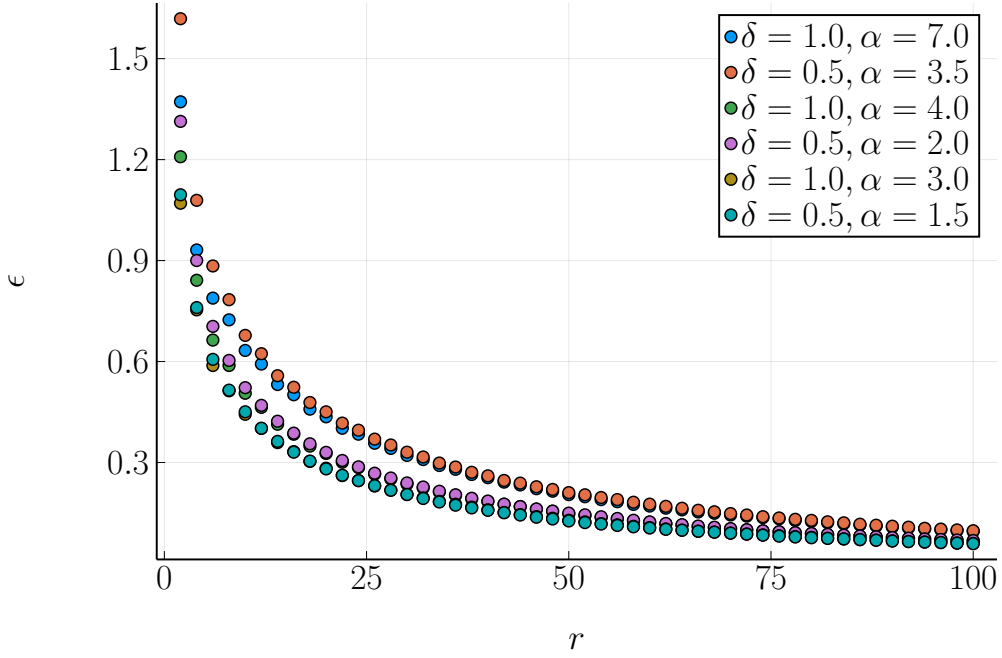


(a) Scaling of the logarithmic negativity, XX, OBC

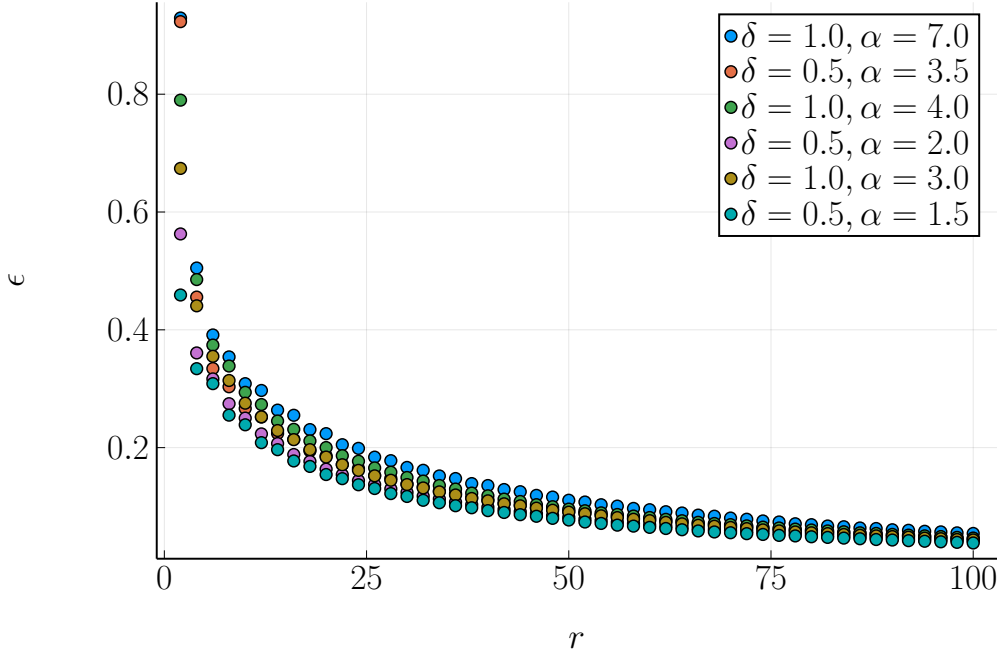


(b) Scaling of the logarithmic negativity, XXY (\(\Delta = 1\)), OBC

Figure 8.3: Scaling of the logarithmic negativity of the open power-law system. In each figure we calculate the negativity over 50,000 disorder realisations whilst keeping  $\alpha = 1, \delta = 1$ . Figure 8.3a: logarithmic negativity for the XX chain. Figure 8.3b: logarithmic negativity for the XXY  $\Delta = 1$  chain. Notice that in each subfigure, the  $L = 2000$  curve is shifted upwards relative to the  $L = 1000$  curve.



(a) Logarithmic negativity with varying  $r$ , XX, OBC. Notice in this case that there is a data collapse for small  $r$  onto the ratio  $\alpha/\delta$ .



(b) Logarithmic negativity with varying  $r$ , XXY ( $\Delta = 1$ ), OBC. Notice in this case that there is no obvious data collapse for small  $r$ .

Figure 8.4: Scaling of the logarithmic negativity of the open  $XX$  and  $XXY$  power-law systems as  $r$  is varied. We restrict  $r$  to even intervals and the position is the same as per figure 7.2.  $L = 1000$  and  $l = 100$  in both figures. We notice that the logarithmic negativity decays very quickly compared to the non-interacting randbow case, figure 7.2a.

## 9 Conclusion

In this report we have confirmed some key findings in the literature on entanglement scaling in random systems, as well as exploring new measures and new systems (e.g. the power-law system). In this section, we will summarise our results and consider some directions for future work.

### 9.1 Logarithmic negativity for the Randbow system

In section 7 we showed that the scaling of the logarithmic negativity of the randbow chain was almost identical to the scaling of the entanglement entropy. In the non-interacting,  $XX$  case, we observe a square root scaling that corresponds to the  $XX$  case for the entanglement entropy. For the interacting  $XXY$  case, we see that the entanglement entropy quickly saturates, which reflects the stability of the bubble regions in this regime. We similarly note that for fixed subsystem sizes but increase intervals  $r$ , the negativity of the interacting model scales far more quickly than the non-interacting model, which is a corollary of the previous result.

### 9.2 Entanglement scaling for the power-law system

For a system with couplings distributed according to a power-law, the scaling of the entanglement entropy and the logarithmic negativity changes significantly. The entanglement entropy at first scales quickly with  $l$ , as the short rainbow phase dominates and effects a volume law. However, this rainbow phase is very unstable due to the relatively slow decaying of the couplings, and from that point onwards a logarithmic scaling is observed, in line with the simple disordered model. This was corroborated with the scaling of the exact case for a smaller system size.

For the logarithmic negativity, we observed that the power-law system scales as expected in a very similar way to the simple disordered system. This still displays an area law violation.

### 9.3 Limitations and Future Work

We have confirmed that area law violations can be achieved even in systems with less spatial inhomogeneity than exponentially decaying randbow model. This contributes another step in our understanding of one dimensional quantum complex system. However, we were not able to establish any strong analytical results for the power-law system. This is not necessarily intractable given more time, but the power-law expression is not as analytically useful as the exponential expression, so any solution will probably not take the same form as the details of [2]. One could also argue that a better, more rigorous argument for the square root scaling of the randbow entanglement entropy is needed, but the data match very well to the heuristic used here and in [2] that we do need see this as being as important as any sort of quantitative theory of power-law systems in general.

A more exhaustive treatment could have been made of the different ways of measuring the entanglement entropy and logarithmic negativity of the power-law system - for example, calculating the exact solution for the entanglement entropy calculations for a different value of  $\alpha/\delta$ . However, we have managed to present the main results and we plan on publishing the tools used for these experiments so that they can be verified later if necessary.

In our opinion, the biggest unmet need in this scheme of work is a physical explanation for the breakdown of the area law violation when we consider the interacting case of the randbow and power-law systems. Whilst in [2] there is a good quantitative argument given in terms of projecting the SDRG procedure onto a random walk, it remains the case that we do not have a clear understanding of what happens locally in the  $\Delta = 1$  case (furthermore, we have not considered values of  $\Delta$  outside of 0 and 1, which could also be the subject of future work). Given that the interactions take us back into an area law phase, which we know is the result of strictly local Hamiltonians, it suggests that the interacting systems could be mapped into a strictly local system for large  $l$  and that that could give some further insight.



## A Quantum Mechanics: A Brief Summary

Quantum mechanics is built on *state vectors* that have a different notion of state to classical state vectors. In a classical system, a state  $s(t)$  at time  $t$  describes how the system would be observed if an experiment were conducted at time  $t$ . The mapping of moments in time to experimental outcomes is one to one: this grounds the idea of *information* in classical mechanics. To have information about the state of a system means that you know what result you will get if you observe the system.

However, in quantum mechanics, the mapping of states to experiment outcomes is now one to many. A *quantum state* does not, in general, tell us what state we will observe the system in at  $t$  - rather, it encodes a range of possible states that the system could be in when observations are drawn from experiment. The result of the experiment will not be known until the experiment has taken place.

### A.1 States and Amplitudes

To demonstrate, we will start with a quantum state  $\psi$  that can be ‘observed’ in two possible outcomes: yes and no.  $\psi$  is a vector in  $\mathbb{C}^2$ , and  $\psi(x)$  is the *probability amplitude* of finding  $\psi$  in state  $x$ . The probability amplitude is the working data of a quantum system; the probability that  $\psi$  is in state  $x$  is  $|\psi(x)|^2$ . We will represent yes with the vector  $y$  and no with the vector  $n$ . The ‘overlap’ of  $\psi$  on the state yes is the inner product  $(y, \psi)$ , and the probability that  $\psi$  is in state  $y$  when observed is  $|(y, \psi)|^2$ .

Because the inner product form occurs so frequently, and because it is helpful to distinguish between column vectors and complex conjugated row vectors, we will use bra and ket form:

$$\psi = |\psi\rangle \quad (\text{A.1})$$

$$\psi' = \langle\psi| \quad (\text{A.2})$$

When  $|\psi\rangle$  is describing a single particle in space, and especially when it is time dependent, it is generally called a *wave function*. This is because the state vector  $|\psi\rangle$  describes a matter wave (of probability amplitude) in space.

The space of quantum states is a *vector space*. For example, a state could be equal proportions yes and no. This is the idea of *superposition*, the quantum phenomenon of objects being in two states (e.g. places) at once. It is often helpful for this space to be given an orthogonal basis, where ‘states’ in the classical sense are represented by orthogonal vectors. For example, in  $\mathbb{C}^2$ , we could have the basis  $\{|y\rangle, |n\rangle\}$ , and a vector could be  $\frac{1}{\sqrt{2}}(|y\rangle + |n\rangle)$ , equally yes and no.

We will also use *density matrices* throughout this work, where the density matrix  $\rho$  of a state is the matrix:

$$\rho = |\psi\rangle\langle\psi| \quad (\text{A.3})$$

### A.2 Normalisation and Unitary Operators

However, for the system to be meaningfully probabilistic, the probabilities associated with each state must be normalised, i.e.:

$$\sum_x ||\psi(x)\rangle|^2 = 1 \quad (\text{A.4})$$

This in turn implies that any function that updates the state of our system from time 0 to time  $t$  must maintain the normalisation condition. This suggests that such a map  $U$  must be norm preserving and thus orthogonal, which in *mathbb{C}^n* means:

$$UU^* = U^*U = I \quad (\text{A.5})$$

That is, the map is unitary.

### A.3 Time Evolution

We will give a brief, intuitive derivation of the Schrödinger equation<sup>5</sup>. For a time dependent system, we have:

$$U(t) |\psi(0)\rangle = |\psi(t)\rangle \quad (\text{A.6})$$

Now assuming that  $U$  can be expanded to first order, we can for small  $\epsilon$  say:

$$U(\epsilon) = I + O(\epsilon) = I - i\epsilon H \quad (\text{A.7})$$

where we have introduced the prefactor  $-i\epsilon$  in front of  $H$  for convenience.  $H$  is thus the first order expansion of  $U(t)$  without the prefactors.

Bringing this all together with the definition of  $U$  in equation A.6, we have:

$$|\psi(\epsilon)\rangle = U(\epsilon) |\psi(0)\rangle = |\psi(0)\rangle - i\epsilon H |\psi(0)\rangle \quad (\text{A.8})$$

Rearranging and dividing by  $\epsilon$ , and relaxing the assumption that our state started at time 0 we have

$$\lim_{\epsilon \rightarrow 0} \frac{|\psi(\epsilon)\rangle - |\psi(0)\rangle}{\epsilon} = \frac{\delta |\psi\rangle}{\delta t} = -iH |\psi\rangle \quad (\text{A.9})$$

This is the time independent Schrödinger equation, which will be useful in section ?? .  $H$  is the Hamiltonian of the system, which will be discussed further in section A.5.

### A.4 Observables

Given a state  $|\psi\rangle$ , we generally want to know something about it - for example, its position, momentum, spin, energy, etc.. In quantum mechanics we use *observables* to extract these from states. Observables are represented by Hermitian linear operators<sup>6</sup>, and their eigenvalues are the values that we can observe through experiment.

The combination of linear operators and vector spaces of states gives rise to the following useful summary<sup>7</sup>:

Properties of a Hermitian Operator	Properties of an Observable $A$
All the eigenvalues of the operator are real.	The values of the observable are real.
The eigenvectors of the operator are orthogonal.	The states of an observable are distinct.
The eigenvectors form a basis for the state space.	The possible values of the observable cover all of the possible values that could be observed for this system.

### A.5 Hamiltonians and Groundstates

In section A.3, we defined the Hamiltonian  $H$  as part of our approximation of the time evolution operator  $U$ . The Hamiltonian is the observable for the total energy of the system. In dynamical systems, this will normally have a kinetic and potential term, but in this report it will focus mostly on the states of spins (see A.7 and 4.1).

The 'solution' to most physical problems is to find the *groundstate*  $|\psi\rangle$  that minimises the energy. That is equivalent to solving the following minimisation problem:

$$\begin{aligned} \min_{|\psi\rangle} \quad & E \\ \text{s.t.} \quad & H |\psi\rangle = E |\psi\rangle \end{aligned} \quad (\text{A.10})$$

<sup>5</sup>The following derivation of the Schrödinger equation is heavily indebted to Susskind [49]. For a more thorough review, see [50].

<sup>6</sup>It is often asserted that such operators must be Hermitian, i.e.  $H = H^\dagger$ , but this is not strictly true: see [51]. Superficially, the requirement is that the operator  $H$  on a space of dimension  $N$  have  $N$  orthogonal eigenvectors and  $N$  real (possibly degenerate) eigenvalues. Hermiticity guarantees this, hence it is a useful requirement to impose.

<sup>7</sup>This summary is taken almost directly from Cresser [52].

## A.6 Commutators

Most operators do not commute, and the same is true within quantum mechanics. We define the *commutator*:

$$[A, B] = AB - BA \quad (\text{A.11})$$

The *anti-commutator* is defined as:

$$\{A, B\} = AB + BA \quad (\text{A.12})$$

Commutation relations are important in defining the relationships between operators. For example, given the position operators  $\hat{x}$  and the momentum operator  $\hat{p}$ :

$$[\hat{x}, \hat{p}] = i\hbar \mathbb{I} \quad (\text{A.13})$$

This relation between two operators that are Fourier transforms of one another is often referred to as the canonical commutation relation.

## A.7 Spin

*Spin* is a form of angular momentum inherent to quantum particles. Spin can be measured in the three different dimensions of normal space, and particles each possess a *spin quantum number*  $s$ . Restrictions on this spin quantum number imply important properties about different quantum particles. Spin is quantized and takes the form:

$$S = \hbar \sqrt{s(s+1)} \quad (\text{A.14})$$

Where  $s$  can be any half-integer. Particles with half-integer spin are *fermions* and particles with integer spins are called *bosons*.

An important property of fermions is that they obey the Pauli Exclusion Principle<sup>[53]</sup>. Consider a *creation operator*  $a_i^\dagger$  that acts on a vacuum state  $|0\rangle$  to create a particle at position  $i$ <sup>8</sup>. Adding a particle at position  $i$  and another at position  $j$  must give us the same state, up to a prefactor:

$$a_i^\dagger a_j^\dagger = \lambda a_j^\dagger a_i^\dagger \quad (\text{A.15})$$

Restricting ourselves without loss of generality to the cases  $\pm 1$ , we consider the bosonic case of  $+1$  first, which implies that *the state vector is symmetric under particle exchange*. This also implies that:

$$a_i^\dagger a_j^\dagger - a_j^\dagger a_i^\dagger = [a_i^\dagger, a_j^\dagger] = 0 \quad (\text{A.16})$$

However, for the *fermionic* case, we have the prefactor  $-1$  and instead the anti-commutator  $\{c_i^\dagger, c_j^\dagger\} = 0$ , where  $c_i^\dagger$  is the fermionic creation operator at  $i$ . Mostly importantly, if we set  $i = j$  then:

$$c_i^\dagger c_i^\dagger + c_i^\dagger c_i^\dagger = 0 \quad (\text{A.17})$$

$$c_i^\dagger c_i^\dagger = 0 \quad (\text{A.18})$$

Which is exactly the Pauli Exclusion Principle: if we try to create two fermions at the same position, they annihilate and we get nothing at all. This will be relevant when we discuss the Jordan-Wigner transformation.

---

<sup>8</sup>This explanation of the exclusion principle is due to Blundell and Lancaster <sup>[50]</sup>.

## B Exact Solution to Non-Interacting Case

### B.1 The Jordan-Wigner Transformation

The Jordan-Wigner (JW) transformation maps a system of spins into a system of (free) fermions. This is useful as it opens up a wider variety of techniques for dealing with disordered, many body problems. We recommend [quantum'ising'beginners] for a thorough overview, and our summary of the JW transformation relies heavily on their layout.

Recall from A.7 that a fermion obeys the Pauli exclusion principle and that one can define a creation operator  $\langle c_i^\dagger \rangle$  with anti-commutator  $\{c_i^\dagger, c_j^\dagger\} = 0$ . Using this, we can say that the JW transformation maps spins to fermions according to the following transformations:

$$\hat{\sigma}_j^x = \hat{K}_j (\hat{c}_j^\dagger + \hat{c}_j) \quad (\text{B.1})$$

$$\hat{\sigma}_j^y = \hat{K}_j i (\hat{c}_j^\dagger - \hat{c}_j) \quad (\text{B.2})$$

$$\hat{\sigma}_j^z = 1 - 2\hat{n}_j \quad (\text{B.3})$$

where  $\hat{n}_j = \hat{c}_j^\dagger \hat{c}_j$  is the fermionic number operator and  $\hat{K}_j = \prod_{j'=1}^{j-1} (1 - 2\hat{n}_{j'})$  is a parity adjusting operator. The physical picture here is that we have gone from spins that can be ‘up or down’ to fermions that can be present or not.

These mappings can be reversed, following [1]:

$$c_i = \left( \prod_{m=1}^{i-1} \sigma_m^z \right) \frac{\sigma_i^x - i\sigma_i^y}{2} \quad (\text{B.4})$$

In the following section we show how this technique can be used to solve the random inhomogeneous chain.

### B.2 Using the JW transformation in the exact solution

Again following [1], we define a slightly more general Hamiltonian than equation 4.1 as follows:

$$H_{XX} = \sum_i J_i (S_i^x S_{i+1}^x + S_i^y S_{i+1}^y) + h \sum_i S_i^z \quad (\text{B.5})$$

Note that this applies strictly to the  $XX$  chain, and the additional  $h$  term. Using equation B.4 this is immediately transformed into a fermionic form:

$$\mathcal{H}_{XX} = \frac{1}{2} \sum_{i=1}^{L-1} J_i (c_i^\dagger c_{i+1} + c_{i+1}^\dagger c_i) + \frac{h}{2} \sum_{i=1}^{L-1} c_i^\dagger c_i \quad (\text{B.6})$$

where we have defined the additional anti-commutator relation  $\{c_m, c_n^\dagger\} = \delta_{m,n}$ .

One can now assume that each new fermion has individual eigenstates of the form:

$$\eta_q^\dagger |0\rangle = \sum_i \Phi_q(i) c_i^\dagger |0\rangle \quad (\text{B.7})$$

where  $q$  labels the different eigenstates and  $\Phi$  is a vector of amplitudes to be found. The Schrödinger equation becomes:

$$J_i \Phi_q(i+1) + J_{i-1} \Phi_q(i-1) = 2\epsilon_q \Phi_q(i) \quad (\text{B.8})$$

where  $\epsilon_q$  are single particle eigenvalues per eigenstates  $q$ . This is a new eigenvalue problem for a banded  $2L \times 2L$  matrix with the couplings  $J_i$  on the off diagonals.

The groundstate of the original Hamiltonian will have  $L \div 2$  fermions, giving us the following:

$$|GS\rangle = \eta_{q_M}^\dagger \eta_{q_{M-1}}^\dagger \cdots \eta_{q_1}^\dagger |0\rangle \quad (\text{B.9})$$

Multiplying equation B.7 by the relevant operators, we can derive the anti-commutators:

$$\{\eta_q^\dagger, c_j^\dagger\} = \{\eta_q, c_j\} = 0 \quad (\text{B.10})$$

and

$$\{\eta_q^\dagger, c_j\} = \Phi_q(j)\delta_{k,j}, \quad \{\eta_q, c_j^\dagger\} = \Phi^*(j)\delta_{k,j} \quad (\text{B.11})$$

Combining the previous two equations, we can derive the two point function's expected value for the groundstate of the original Hamiltonian:

$$\langle c_i^\dagger c_j \rangle = \sum_q \Phi_q^*(i) \Phi_q(j) \quad (\text{B.12})$$

This defines a matrix  $C_{i,j}$  that can be restricted to some subsystem  $A$  for the purposes of analysing a given disorder realisation. In particular, from [54], we can calculate the entanglement entropy:

$$S_A = - \sum_l (\lambda_k \ln \lambda_k + (1 - \lambda_k) \ln (1 - \lambda_k)) \quad (\text{B.13})$$

This completes our overview of the technique used in 6.5 to calculate the entanglement entropy of the randbow chain exactly.

## References

- [1] Paola Ruggiero, Vincenzo Alba, and Pasquale Calabrese. “The Entanglement Negativity in Random Spin Chains”. May 2, 2016. DOI: [10.1103/PhysRevB.94.035152](https://doi.org/10.1103/PhysRevB.94.035152). arXiv: [1605.00674](https://arxiv.org/abs/1605.00674). URL: <http://arxiv.org/abs/1605.00674>.
- [2] Vincenzo Alba et al. “Unusual Area-Law Violation in Random Inhomogeneous Systems”. In: *Journal of Statistical Mechanics: Theory and Experiment* 2019.2 (Feb. 26, 2019), p. 023105. ISSN: 1742-5468. DOI: [10.1088/1742-5468/ab02df](https://doi.org/10.1088/1742-5468/ab02df). URL: <https://iopscience.iop.org/article/10.1088/1742-5468/ab02df>.
- [3] Alexander A. Tsirlin et al. “Spiral Ground State in the Quasi-Two-Dimensional Spin-1/2 System Cu<sub>2</sub>GeO<sub>4</sub>”. Sept. 16, 2010. DOI: [10.1103/PhysRevB.83.104415](https://doi.org/10.1103/PhysRevB.83.104415). arXiv: [1009.3287](https://arxiv.org/abs/1009.3287). URL: <http://arxiv.org/abs/1009.3287> (visited on 08/18/2022).
- [4] Paola Ruggiero and Pasquale Calabrese. *Entanglement and Correlations in One-Dimensional Quantum Many-Body Systems*. Trieste: SCUOLA INTERNAZIONALE SUPERIORE DI STUDI AVANZATI, 2019.
- [5] Jordi Molins. “Long Range Ising Model for Credit Risk Modeling”. In: *AIP Conference Proceedings*. Vol. 779. AIP, July 20, 2005, pp. 156–161. ISBN: 0-7354-0266-3. DOI: [10.1063/1.2008607](https://doi.org/10.1063/1.2008607). URL: <http://aip.scitation.org/doi/abs/10.1063/1.2008607>.
- [6] Lars Onsager. “A Two-Dimensional Model with an Order-Disorder Transition”. In: *Physical Review* 65.3-4 (Feb. 1, 1944), p. 117. ISSN: 0031899X. DOI: [10.1103/PhysRev.65.117](https://doi.org/10.1103/PhysRev.65.117). URL: <https://journals.aps.org/pr/abstract/10.1103/PhysRev.65.117> (visited on 08/21/2022).
- [7] G. Refael and J. E. Moore. “Entanglement Entropy of Random Quantum Critical Points in One Dimension”. In: *Physical Review Letters* 93 (26 I June 29, 2004). DOI: [10.1103/PhysRevLett.93.260602](https://doi.org/10.1103/PhysRevLett.93.260602). arXiv: [cond-mat/0406737](https://arxiv.org/abs/cond-mat/0406737). URL: <http://arxiv.org/abs/cond-mat/0406737>.
- [8] M. B. Hastings. “An Area Law for One Dimensional Quantum Systems”. May 14, 2007. DOI: [10.1088/1742-5468/2007/08/P08024](https://doi.org/10.1088/1742-5468/2007/08/P08024). arXiv: [0705.2024](https://arxiv.org/abs/0705.2024). URL: <http://arxiv.org/abs/0705.2024> (visited on 08/18/2022).
- [9] G Vitagliano, A Riera, and J I Latorre. “Volume-Law Scaling for the Entanglement Entropy in Spin-1/2 Chains”. In: *New Journal of Physics* 12.11 (Nov. 26, 2010), p. 113049. ISSN: 1367-2630. DOI: [10.1088/1367-2630/12/11/113049](https://doi.org/10.1088/1367-2630/12/11/113049). URL: <https://iopscience.iop.org/article/10.1088/1367-2630/12/11/113049>.
- [10] J. Eisert, M. Cramer, and M. B. Plenio. “Area Laws for the Entanglement Entropy”. In: *Reviews of Modern Physics* 82.1 (Feb. 4, 2010), pp. 277–306. ISSN: 0034-6861. DOI: [10.1103/RevModPhys.82.277](https://doi.org/10.1103/RevModPhys.82.277). arXiv: [0808.3773](https://arxiv.org/abs/0808.3773). URL: <https://link.aps.org/doi/10.1103/RevModPhys.82.277>.
- [11] Don N. Page. “Information in Black Hole Radiation”. In: *Physical Review Letters* 71.23 (Dec. 6, 1993), p. 3743. ISSN: 00319007. DOI: [10.1103/PhysRevLett.71.3743](https://doi.org/10.1103/PhysRevLett.71.3743). arXiv: [hep-th/9306083](https://arxiv.org/abs/hep-th/9306083). URL: <https://journals.aps.org/prl/abstract/10.1103/PhysRevLett.71.3743> (visited on 08/24/2022).
- [12] Jean Zinn-Justin. “Mean Field Theory For Ferromagnetic Systems”. In: *Quantum Field Theory and Critical Phenomena*. Oxford University Press, June 6, 2002, pp. 592–615. DOI: [10.1093/acprof:oso/9780198509233.003.0024](https://doi.org/10.1093/acprof:oso/9780198509233.003.0024). URL: <https://academic.oup.com/book/11638/chapter/160554734> (visited on 08/19/2022).
- [13] Daniel S. Fisher. “Random Antiferromagnetic Quantum Spin Chains”. In: *Physical Review B* 50.6 (Aug. 1, 1994), pp. 3799–3821. ISSN: 0163-1829. DOI: [10.1103/PhysRevB.50.3799](https://doi.org/10.1103/PhysRevB.50.3799). URL: <https://link.aps.org/doi/10.1103/PhysRevB.50.3799>.
- [14] Luca Bombelli et al. “Quantum Source of Entropy for Black Holes”. In: *Physical Review D* 34.2 (July 15, 1986), pp. 373–383. ISSN: 0556-2821. DOI: [10.1103/PhysRevD.34.373](https://doi.org/10.1103/PhysRevD.34.373). URL: <https://link.aps.org/doi/10.1103/PhysRevD.34.373>.

- [15] Mark Srednicki. “Entropy and Area”. In: *Physical Review Letters* 71.5 (Aug. 2, 1993), pp. 666–669. ISSN: 0031-9007. DOI: [10.1103/PhysRevLett.71.666](https://doi.org/10.1103/PhysRevLett.71.666). arXiv: [hep-th/9303048v2](https://arxiv.org/abs/hep-th/9303048v2). URL: <https://link.aps.org/doi/10.1103/PhysRevLett.71.666> (visited on 08/20/2022).
- [16] M. B. Plenio et al. “Entropy, Entanglement, and Area: Analytical Results for Harmonic Lattice Systems”. In: *Physical Review Letters* 94.6 (Feb. 17, 2005), p. 060503. ISSN: 0031-9007. DOI: [10.1103/PhysRevLett.94.060503](https://doi.org/10.1103/PhysRevLett.94.060503). arXiv: [quant-ph/0405142v3](https://arxiv.org/abs/quant-ph/0405142v3). URL: <https://link.aps.org/doi/10.1103/PhysRevLett.94.060503> (visited on 08/21/2022).
- [17] J. Eisert, M. Cramer, and M. B. Plenio. “Colloquium: Area Laws for the Entanglement Entropy”. In: *Reviews of Modern Physics* 82.1 (Feb. 4, 2010), pp. 277–306. ISSN: 00346861. DOI: [10.1103/REVMODPHYS.82.277/FIGURES/2/MEDIUM](https://doi.org/10.1103/REVMODPHYS.82.277/FIGURES/2/MEDIUM). URL: <https://journals.aps.org/rmp/abstract/10.1103/RevModPhys.82.277> (visited on 08/24/2022).
- [18] Michael M. Wolf. “Violation of the Entropic Area Law for Fermions”. In: *Physical Review Letters* 96.1 (Jan. 13, 2006), p. 010404. ISSN: 10797114. DOI: [10.1103/PHYSREVLETT.96.010404/FIGURES/1/MEDIUM](https://doi.org/10.1103/PHYSREVLETT.96.010404/FIGURES/1/MEDIUM). arXiv: [quant-ph/0503219](https://arxiv.org/abs/quant-ph/0503219). URL: <https://journals.aps.org/prl/abstract/10.1103/PhysRevLett.96.010404> (visited on 08/24/2022).
- [19] Pasquale Calabrese and John Cardy. “Entanglement Entropy and Quantum Field Theory”. In: *Journal of Statistical Mechanics: Theory and Experiment* 2004.06 (June 12, 2004), P06002. ISSN: 1742-5468. DOI: [10.1088/1742-5468/2004/06/P06002](https://doi.org/10.1088/1742-5468/2004/06/P06002). URL: <https://iopscience.iop.org/article/10.1088/1742-5468/2004/06/P06002> (visited on 08/18/2022).
- [20] Don N. Page. “Average Entropy of a Subsystem”. In: *Physical Review Letters* 71.9 (Aug. 30, 1993), pp. 1291–1294. ISSN: 0031-9007. DOI: [10.1103/PhysRevLett.71.1291](https://doi.org/10.1103/PhysRevLett.71.1291). arXiv: [gr-qc/9305007v2](https://arxiv.org/abs/gr-qc/9305007v2). URL: <https://link.aps.org/doi/10.1103/PhysRevLett.71.1291> (visited on 08/20/2022).
- [21] Salvatore Marco Giampaolo, Flavia Brága Ramos, and Fabio Franchini. “The Frustration of Being Odd: Universal Area Law Violation in Local Systems”. In: *Journal of Physics Communications* 3.8 (Aug. 1, 2019), p. 081001. ISSN: 2399-6528. DOI: [10.1088/2399-6528/ab3ab3](https://doi.org/10.1088/2399-6528/ab3ab3). URL: <https://iopscience.iop.org/article/10.1088/2399-6528/ab3ab3> (visited on 08/21/2022).
- [22] Pasquale Calabrese, John Cardy, and Erik Tonni. “Entanglement Negativity in Quantum Field Theory”. In: *Physical Review Letters* 109.13 (Sept. 28, 2012), p. 130502. ISSN: 0031-9007. DOI: [10.1103/PhysRevLett.109.130502](https://doi.org/10.1103/PhysRevLett.109.130502). arXiv: [1206.3092](https://arxiv.org/abs/1206.3092). URL: <https://link.aps.org/doi/10.1103/PhysRevLett.109.130502> (visited on 08/20/2022).
- [23] Luigi Amico et al. “Entanglement in Many-Body Systems”. In: *Reviews of Modern Physics* 80.2 (May 6, 2008), pp. 517–576. ISSN: 0034-6861. DOI: [10.1103/RevModPhys.80.517](https://doi.org/10.1103/RevModPhys.80.517). URL: <https://link.aps.org/doi/10.1103/RevModPhys.80.517>.
- [24] J. S. Bell. “On the Einstein Podolsky Rosen Paradox”. In: *Physics Physique Fizika* 1.3 (Nov. 1, 1964), pp. 195–200. ISSN: 0554-128X. DOI: [10.1103/PhysicsPhysiqueFizika.1.195](https://doi.org/10.1103/PhysicsPhysiqueFizika.1.195). URL: <https://link.aps.org/doi/10.1103/PhysicsPhysiqueFizika.1.195> (visited on 08/21/2022).
- [25] John F. Clauser et al. “Proposed Experiment to Test Local Hidden-Variable Theories”. In: *Physical Review Letters* 23.15 (Oct. 13, 1969), p. 880. ISSN: 00319007. DOI: [10.1103/PhysRevLett.23.880](https://doi.org/10.1103/PhysRevLett.23.880). URL: <https://journals.aps.org/prl/abstract/10.1103/PhysRevLett.23.880> (visited on 08/21/2022).
- [26] V. Vedral et al. “Quantifying Entanglement”. In: *Physical Review Letters* 78.12 (Mar. 24, 1997), p. 2275. ISSN: 10797114. DOI: [10.1103/PhysRevLett.78.2275](https://doi.org/10.1103/PhysRevLett.78.2275). arXiv: [quant-ph/9702027](https://arxiv.org/abs/quant-ph/9702027). URL: <https://journals.aps.org/prl/abstract/10.1103/PhysRevLett.78.2275> (visited on 08/21/2022).
- [27] N. Gisin. “Hidden Quantum Nonlocality Revealed by Local Filters”. In: *Physics Letters A* 210.3 (Jan. 1996), pp. 151–156. ISSN: 03759601. DOI: [10.1016/S0375-9601\(96\)80001-6](https://doi.org/10.1016/S0375-9601(96)80001-6). URL: <https://linkinghub.elsevier.com/retrieve/pii/S0375960196800016>.



- [28] M. B. Plenio. “Logarithmic Negativity: A Full Entanglement Monotone That Is Not Convex”. In: *Physical Review Letters* 95.9 (Aug. 26, 2005), p. 090503. ISSN: 0031-9007. DOI: [10.1103/PhysRevLett.95.090503](https://doi.org/10.1103/PhysRevLett.95.090503). URL: <https://link.aps.org/doi/10.1103/PhysRevLett.95.090503> (visited on 08/21/2022).
- [29] Charles H. Bennett et al. “Mixed-State Entanglement and Quantum Error Correction”. In: *Physical Review A* 54.5 (Nov. 1, 1996), pp. 3824–3851. ISSN: 1050-2947. DOI: [10.1103/PhysRevA.54.3824](https://doi.org/10.1103/PhysRevA.54.3824). URL: <https://link.aps.org/doi/10.1103/PhysRevA.54.3824>.
- [30] Pasquale Calabrese and Alexandre Lefevre. “Entanglement Spectrum in One-Dimensional Systems”. In: *Physical Review A* 78.3 (Sept. 23, 2008), p. 032329. ISSN: 1050-2947. DOI: [10.1103/PhysRevA.78.032329](https://doi.org/10.1103/PhysRevA.78.032329). arXiv: [0806.3059](https://arxiv.org/abs/0806.3059). URL: <https://link.aps.org/doi/10.1103/PhysRevA.78.032329> (visited on 08/22/2022).
- [31] Michael E. Fisher. “Renormalization Group Theory: Its Basis and Formulation in Statistical Physics”. In: *Reviews of Modern Physics* 70.2 (Apr. 1, 1998), pp. 653–681. ISSN: 0034-6861. DOI: [10.1103/RevModPhys.70.653](https://doi.org/10.1103/RevModPhys.70.653). URL: <https://link.aps.org/doi/10.1103/RevModPhys.70.653>.
- [32] Ferenc Igloi and Cecile Monthus. “Strong Disorder RG Approach of Random Systems”. Feb. 18, 2005. DOI: [10.1016/j.physrep.2005.02.006](https://doi.org/10.1016/j.physrep.2005.02.006). arXiv: [cond-mat/0502448](https://arxiv.org/abs/cond-mat/0502448). URL: <http://arxiv.org/abs/cond-mat/0502448>.
- [33] Ferenc Igloi and Cécile Monthus. “Strong Disorder RG Approach – a Short Review of Recent Developments”. In: *European Physical Journal B* 91.11 (2018). ISSN: 14346036. DOI: [10.1140/epjb/e2018-90434-8](https://doi.org/10.1140/epjb/e2018-90434-8). arXiv: [1806.07684](https://arxiv.org/abs/1806.07684).
- [34] Barry M. McCoy and Tai Tsun Wu. “Theory of a Two-Dimensional Ising Model with Random Impurities. I. Thermodynamics”. In: *Physical Review* 176.2 (Dec. 10, 1968), pp. 631–643. ISSN: 0031-899X. DOI: [10.1103/PhysRev.176.631](https://doi.org/10.1103/PhysRev.176.631). URL: <https://link.aps.org/doi/10.1103/PhysRev.176.631>.
- [35] Shang-keng Ma, Chandan Dasgupta, and Chin-kun Hu. “Random Antiferromagnetic Chain”. In: *Physical Review Letters* 43.19 (Nov. 5, 1979), pp. 1434–1437. ISSN: 0031-9007. DOI: [10.1103/PhysRevLett.43.1434](https://doi.org/10.1103/PhysRevLett.43.1434). URL: <https://link.aps.org/doi/10.1103/PhysRevLett.43.1434>.
- [36] Chandan Dasgupta and Shang-keng Ma. “Low-Temperature Properties of the Random Heisenberg Antiferromagnetic Chain”. In: *Physical Review B* 22.3 (Aug. 1, 1980), pp. 1305–1319. ISSN: 0163-1829. DOI: [10.1103/PhysRevB.22.1305](https://doi.org/10.1103/PhysRevB.22.1305). URL: <https://link.aps.org/doi/10.1103/PhysRevB.22.1305>.
- [37] Jean-Philippe Bouchaud and Antoine Georges. “Anomalous Diffusion in Disordered Media: Statistical Mechanisms, Models and Physical Applications”. In: *Physics Reports* 195.4-5 (Nov. 1990), pp. 127–293. ISSN: 03701573. DOI: [10.1016/0370-1573\(90\)90099-N](https://doi.org/10.1016/0370-1573(90)90099-N). URL: <https://linkinghub.elsevier.com/retrieve/pii/037015739090099N>.
- [38] Olexei Motrunich et al. “Infinite-Randomness Quantum Ising Critical Fixed Points”. In: *Physical Review B - Condensed Matter and Materials Physics* 61.2 (June 21, 1999), pp. 1160–1172. DOI: [10.1103/PhysRevB.61.1160](https://doi.org/10.1103/PhysRevB.61.1160). arXiv: [cond-mat/9906322v1](https://arxiv.org/abs/cond-mat/9906322v1). URL: <http://arxiv.org/abs/cond-mat/9906322> (visited on 08/22/2022).
- [39] C. Monthus. “On the Localization of Random Heteropolymers at the Interface between Two Selective Solvents”. In: *The European Physical Journal B* 13.1 (Jan. 1, 2000), pp. 111–130. ISSN: 1434-6028. DOI: [10.1007/s100510050016](https://doi.org/10.1007/s100510050016). URL: <http://link.springer.com/10.1007/s100510050016>.
- [40] Steven R. White. “Density Matrix Formulation for Quantum Renormalization Groups”. In: *Physical Review Letters* 69.19 (Nov. 9, 1992), p. 2863. ISSN: 00319007. DOI: [10.1103/PhysRevLett.69.2863](https://doi.org/10.1103/PhysRevLett.69.2863). URL: <https://journals.aps.org/prl/abstract/10.1103/PhysRevLett.69.2863> (visited on 08/20/2022).



- [41] U. Schollwöck. “The Density-Matrix Renormalization Group”. In: *Reviews of Modern Physics* 77.1 (Apr. 26, 2005), pp. 259–315. ISSN: 0034-6861. DOI: [10.1103/RevModPhys.77.259](https://doi.org/10.1103/RevModPhys.77.259). URL: <https://link.aps.org/doi/10.1103/RevModPhys.77.259> (visited on 08/20/2022).
- [42] Ulrich Schollwoeck. “The Density-Matrix Renormalization Group in the Age of Matrix Product States”. Aug. 20, 2010. DOI: [10.1016/j.aop.2010.09.012](https://doi.org/10.1016/j.aop.2010.09.012). arXiv: [1008.3477](https://arxiv.org/abs/1008.3477). URL: <http://arxiv.org/abs/1008.3477> (visited on 08/22/2022).
- [43] Asher Peres. “Separability Criterion for Density Matrices”. In: *Physical Review Letters* 77.8 (Aug. 19, 1996), pp. 1413–1415. ISSN: 0031-9007. DOI: [10.1103/PhysRevLett.77.1413](https://doi.org/10.1103/PhysRevLett.77.1413). arXiv: [quant-ph/9604005](https://arxiv.org/abs/quant-ph/9604005). URL: <https://link.aps.org/doi/10.1103/PhysRevLett.77.1413> (visited on 08/21/2022).
- [44] Alfréd Rényi. “On Measures of Entropy and Information”. In: *Berkeley Symposium on Mathematical Statistics and Probability* 4 (1961), pp. 547–561.
- [45] Elliott H. Lieb and Mary Beth Ruskai. “Proof of the Strong Subadditivity of Quantum-mechanical Entropy”. In: *Journal of Mathematical Physics* 44.12 (Nov. 3, 2003), p. 1938. ISSN: 0022-2488. DOI: [10.1063/1.1666274](https://doi.org/10.1063/1.1666274). URL: <https://aip.scitation.org/doi/abs/10.1063/1.1666274> (visited on 08/22/2022).
- [46] G. Vidal and R. F. Werner. “Computable Measure of Entanglement”. In: *Physical Review A* 65.3 (Feb. 22, 2002), p. 032314. ISSN: 1050-2947. DOI: [10.1103/PhysRevA.65.032314](https://doi.org/10.1103/PhysRevA.65.032314). URL: <https://link.aps.org/doi/10.1103/PhysRevA.65.032314>.
- [47] Paola Ruggiero and Xhek Turkeshi. “Quantum Information Spreading in Random Spin Chains”. June 6, 2022. DOI: [10.48550/arXiv.2206.02934](https://doi.org/10.48550/arXiv.2206.02934). arXiv: [2206.02934](https://arxiv.org/abs/2206.02934). URL: <http://arxiv.org/abs/2206.02934> (visited on 08/21/2022).
- [48] Maurizio Fagotti, Pasquale Calabrese, and Joel E. Moore. “Entanglement Spectrum of Random-Singlet Quantum Critical Points”. In: *Physical Review B - Condensed Matter and Materials Physics* 83.4 (Jan. 31, 2011), p. 045110. ISSN: 10980121. DOI: [10.1103/PhysRevB.83.045110](https://doi.org/10.1103/PhysRevB.83.045110). arXiv: [1009.1614](https://arxiv.org/abs/1009.1614). URL: <https://journals.aps.org/prb/abstract/10.1103/PhysRevB.83.045110> (visited on 08/25/2022).
- [49] Leonard Susskind. *The Theoretical Minimum - Quantum Mechanics*. 2014. URL: <https://www.youtube.com/playlist?list=PL701CD168D02FF56F> (visited on 08/20/2022).
- [50] Tom Lancaster and Stephen J Blundell. *Quantum Field Theory for the Gifted Amateur*. 5. Oxford: Oxford University Press, 2014. ISBN: 978-0-19-969933-9.
- [51] Carl M Bender. “Introduction to PT-symmetric Quantum Theory”. In: *Contemporary Physics* 46.4 (July 11, 2005), pp. 277–292. ISSN: 0010-7514. DOI: [10.1080/00107500072632](https://doi.org/10.1080/00107500072632). arXiv: [quant-ph/0501052v1](https://arxiv.org/abs/quant-ph/0501052v1). URL: <http://www.tandfonline.com/doi/abs/10.1080/00107500072632> (visited on 08/20/2022).
- [52] J D Cresser. *Quantum Physics Notes*. 2011.
- [53] Wolfgang Pauli. “Exclusion Principle and Quantum Mechanics”. In: (1946).
- [54] Ingo Peschel and Viktor Eisler. “Reduced Density Matrices and Entanglement Entropy in Free Lattice Models”. In: *Journal of Physics A: Mathematical and Theoretical* 42.50 (Dec. 2009), p. 504003. ISSN: 1751-8121. DOI: [10.1088/1751-8121/42/50/504003](https://doi.org/10.1088/1751-8121/42/50/504003). URL: <https://doi.org/10.1088/1751-8121/42/50/504003> (visited on 08/30/2022).